

OBSERVED WAVE DATA: THE SHORE-BREAKER HEIGHT

COASTAL ZONE
INFORMATION CENTER

by

James H. Balsillie

Analysis/Research Section
Bureau of Coastal Data Acquisition
Division of Beaches and Shores
Florida Department of Natural Resources
3900 Commonwealth Blvd., Tallahassee, FL 32303

and

R. W. G. Carter

School of Biological and Environmental Studies
The New University of Ulster
Coleraine, Co. Londonderry, Northern Ireland BT52 1SA U. K.

BEACHES AND SHORES
TECHNICAL AND DESIGN MEMORANDUM NO. 84-2

Reviewed by

Beaches and Shores Resource Center
Institute of Science and Public Affairs
Florida State University

and

Florida Office of Coastal Management
Florida Department of Environmental Regulation

Funded by

A grant from the U. S. Office of Coastal Zone Management
National Oceanic and Atmospheric Administration
(under the Coastal Zone Management Act of 1972, as amended)
through

Florida Office of Coastal Management
Florida Department of Environmental Regulation
and
Florida Department of Natural Resources

FOREWORD

This work presents the description of shore-breaking wave height behavior in terms of the accuracy of visually observed heights compared to measured height information. Various statistical measures related to the shore-breaker height distribution are developed, which are essential in determining and assessing coastal engineering design solutions. In part, this work is essential to the development of a multiple shore-breaking wave transformation model described in subsequent work.

The work described herein constitutes partial fulfillment of contractual obligations with the Federal Coastal Zone Management Program (Coastal Zone Management Act of 1972, as amended) through the Florida Office of Coastal Management subject to provisions of contract CM-37 entitled "Engineering Support Enhancement Program". Under provisions of DNR contract C0037, this work was reviewed by the Beaches and Shores Resource Center, Institute of Science and Public Affairs, Florida State University. The document has been adopted as a Beaches and Shores Technical and Design Memorandum in accordance with provisions of Chapter 16B-33, Florida Administrative Code. Data collection and analytical work were accomplished by the authors prior to initiation of or extemporaneous to this contract. Contractual support for the present work was in the form of final typing, review and editing of the manuscript and drafting of figures.

At the time of submission for contractual compliance, James H. Balsillie was the contract manager and Administrator of the Analysis/Research Section, Hal N. Bean was Chief of the Bureau of Coastal Data Acquisition, Deborah E. Flack Director of the Division of Beaches and Shores, and Dr. Elton J. Gissendanner the Executive Director of the Florida Department of Natural Resources.

Property of CSC Library

Deborah E. Flack

Deborah E. Flack, Director
Division of Beaches and Shores

April, 1984

U. S. DEPARTMENT OF COMMERCE NOAA
COASTAL SERVICES CENTER
2234 SOUTH HOBSON AVENUE
CHARLESTON, SC 29405-2413

GB 459 FS66 708.84-2

11321305

JAN 21 1987

CONTENTS

	Page
INTRODUCTION	1
DATA AND METHODS	3
<u>Visually Observed Shore-Breaker Heights</u>	3
<u>Measured Nearshore Wave Heights</u>	3
MOMENT WAVE HEIGHT STATISTICS	7
<u>Natural Wave Height Variability</u>	9
Spectral Records	9
Single Wave Train Records at Shore-Breaking	11
<u>Relationship between Spectral and Single Wave Train Moment</u> <u>Statistics</u>	20
<u>Over-Estimation of Visual Observations</u>	29
<u>Error Associated with Visual Observations</u>	34
The Psychological Attribute of Size Constancy	34
Cognitive Methodology of Height Estimation	36
An Error Analysis	36
LONG-TERM SHORE-BREAKER HEIGHT DISTRIBUTION AND CLIMATOLOGY	41
<u>Forced Shore-Incident Storm Waves</u>	43
<u>Normally Expected Shore-Breaker Activity</u>	43
<u>Free Shore-Incident Storm Waves</u>	47
CONCLUSIONS	62
ACKNOWLEDGEMENTS	66
REFERENCES	67

OBSERVED WAVE DATA: THE SHORE-BREAKER HEIGHT

by

James H. Balsillie

Analysis/Research Section, Bureau of Coastal Data Acquisition, Division of Beaches and Shores, Florida Department of Natural Resources, 3900 Commonwealth Blvd., Tallahassee, FL 32303.

and

R. W. G. Carter

School of Biological and Environmental Studies, The New University of Ulster, Coleraine, Co. Derry, Northern Ireland BT52 ISA U. K.

INTRODUCTION

The most satisfactory source of nearshore wave information is generally considered to be provided by recording wave gages (McClenan and Harris, 1975). Data from this source provides significant wave heights and corresponding periods from spectra recorded in the nearshore seaward of the surf zone (Harris, 1972). However Balsillie (1980, in manuscripts) has shown that as waves begin to shore-break they can significantly increase in height reaching a maximum at the shore-breaking position. Wave gage data, therefore, may not adequately represent surf zone wave activity since gages are not located in the surf zone where they are "hard pressed" to survive. In addition, the cost of a single wave gage, its installation and maintenance, and data reduction and analysis is not insignificant. Considerable time is also involved in analysis of the spectral records. These factors along with the remoteness of many coastal areas and adverse conditions for gage installation often preclude the use of instrumentation.

An alternate source of nearshore wave data was introduced by Berg (1968) who proposed procedures, using visual estimation techniques, for

inexpensively obtaining nearshore wave information on a routine basis in order to augment and extend amounts of data available for scientific and engineering applications. This program, termed the Littoral Environment Observation (LEO) program, provides for accumulation of data for wave heights, and periods, angle of wave approach to the shoreline, shore-breaker type, longshore current speeds, local wind conditions, beach geometry and occurrence of rip currents. Subsequent to its implementation, the LEO program has been expanded to include sites throughout the United States (Szuwalski, 1977; Bruno and Hiipakka, 1973; Balsillie, 1975a; DeWall and Richter, 1977; Schneider, 1977; Schneider and Weggel, 1980; etc.), and has been adopted elsewhere such as in the Coastal Observation Programme -- Engineering (COPE) in Queensland, Australia (Robinson and Jones, 1977). Data so collected have been used in a variety of empirical investigations (e.g., Balsillie, 1975a, 1975b, 1977a, 1977b; Walton, 1980) for prediction of coastal processes.

Although, as noted, a number of littoral parameters are reported using LEO visual estimation techniques, in this paper the nearshore wave height only is investigated. Advantages of LEO estimation techniques for obtaining nearshore wave height data include: 1. an average wave height can be inexpensively reported for single visual observations which does not involve complex and time consuming spectral analysis required for analysis of gage records, and 2. LEO techniques provide a measure of the shore-breaking wave height which gages cannot. However, throughout the history of the LEO program a number of questions have been understandably asked: 1. what is the accuracy of a single LEO breaker observation, 2. how many LEO breaker height observations are required per extended time period (e.g., a month) to provide results suitable for scientific and engineering applications, and 3. what does the observed breaker height represent in terms

of the wave height distribution? These questions are investigated in this paper.

DATA AND METHODS

In February 1977, a field data collection program was initiated by the authors for obtention of littoral zone data. Thirty-five experiments were completed around Florida's shoreline (Figure 1) at a geographically wide range of localities selected in order to sample the wide range of wave environments found along coastal Florida (Tanner, 1960; Thompson, 1977). A portion of the field data is used in the ensuing investigation, wherein both LEO visual estimations and measured characteristics were obtained. (Table 1).

Visually Observed Shore-Breaking Heights

At the beginning of each field experiment all available participants (between 2 and 8) independently completed a modified LEO reporting form (Figure 2). Each observer was classified on a scale of from 1 to 5 according to the amount of experience each had with observing and reporting littoral conditions. Altogether, a total of 16 observers contributed, with only 3 contributing regularly throughout the experiments. Observers were then divided into 2 groups: experienced (E group) and inexperienced (I group) in order to inspect for any difference in unaided visual estimation competence.

A total of 60 sets of observations were made by the 3 members constituting the E group. Thirty-two observations were obtained by the I group which was composed of a total of 15 individuals, none of whom made more than 5 sets of observations each.


Measured Nearshore Wave Heights

Immediately following visual observations, breaking wave heights were

Table 1. Observed and measured moment wave height statistics.

Exp. No.	Observer	Observed Moment Data	Measured Moment Data		Exp. No.	Observer	Observed Moment Data	Measured Moment Data	
		H _b LEO (m)	H _b (m)	s (m)			H _b LEO (m)	H _b (m)	s (m)
5	J	0.122	0.153	0.0381	16	J	0.366	0.386	0.0386
"	B	0.280	"	"	"	B	0.274	"	"
"	C	0.152	"	"	"	I	0.457	"	"
"	I	0.244	"	"	"	I	0.366	"	"
6	J	0.457	0.351	0.0862	"	I	0.457	"	"
"	B	0.305	"	"	"	I	0.457	"	"
"	C	0.549	"	"	"	I	0.366	"	"
7	J	0.122	0.075	0.0176	17	J	0.305	0.450	0.0929
"	B	0.122	"	"	"	I	0.762	"	"
"	C	0.152	"	"	"	I	0.457	"	"
8	J	0.305	0.228	0.0629	"	I	0.792	"	"
"	B	0.274	"	"	"	I	0.366	"	"
"	C	0.427	"	"	"	I	0.305	"	"
9	J	0.305	0.389	0.1062	18	J	0.274	0.170	0.0372
"	B	0.549	"	"	"	B	0.183	"	"
"	C	0.274	"	"	"	C	0.254	"	"
10	J	0.259	0.199	0.0634	"	J	0.089	0.098	0.0182
"	B	0.305	"	"	"	B	0.061	"	"
"	C	0.244	"	"	"	C	0.122	"	"
"	J	0.396	0.466	0.0996	19	J	0.274	0.171	0.0354
"	B	0.549	"	"	"	B	0.091	"	"
"	C	0.396	"	"	"	C	0.305	"	"
11	J	0.122	0.108	0.0314	"	I	0.701	"	"
"	B	0.122	"	"	"	I	0.305	"	"
"	C	0.152	"	"	"	I	0.305	"	"
13	J	0.122	0.107	0.0309	"	I	0.305	"	"
"	B	0.152	"	"	20	J	0.310	0.115	0.0131
"	I	0.244	"	"	"	B	0.152	"	"
"	I	0.091	"	"	"	C	0.305	"	"
"	I	0.152	"	"	22	B	0.091	0.080	0.0165
"	I	0.213	"	"	"	C	0.091	"	"
"	I	0.244	"	"	23	B	0.274	0.487	0.0701
"	I	0.244	"	"	"	C	0.457	"	"
14	J	0.061	0.056	0.0113	24	B	0.243	0.337	0.0603
"	B	0.061	"	"	"	C	0.457	"	"
"	I	0.091	"	"	25	B	0.254	0.303	0.0584
"	I	0.122	"	"	"	C	0.305	"	"
15	J	0.610	0.541	0.1255	28	J	0.244	0.244	0.0456
"	B	0.610	"	"	"	I	0.610	"	"
"	I	0.457	"	"	"	I	0.451	"	"
"	I	0.610	"	"	"	I	0.450	"	"
"	I	0.488	"	"	29	C	0.762	0.745	0.1695
"	I	0.792	"	"	30	B	1.067	0.850	0.1815
"	I	0.610	"	"	"	C	0.671	"	"
"	I	0.549	"	"	32	J	0.975	0.833	0.1449
"					"	B	0.701	"	"
"					"	C	0.701	"	"

NOTE: J, B and C constitute the E (i.e., experienced) observer group; I the inexperienced observer group.

STATE OF FLORIDA DEPARTMENT OF NATURAL RESOURCES BUREAU OF BEACHES AND SHORES						
FLORIDA LITTORAL ENVIRONMENT OBSERVATIONS RECORD ALL DATA CAREFULLY AND LEGIBLY						
SITE NUMBERS <div style="border: 1px solid black; width: 40px; height: 20px; margin: 0 auto;"></div>	YEAR <div style="border: 1px solid black; width: 40px; height: 20px; margin: 0 auto;"></div>	MONTH <div style="border: 1px solid black; width: 40px; height: 20px; margin: 0 auto;"></div>	DAY <div style="border: 1px solid black; width: 40px; height: 20px; margin: 0 auto;"></div>	Record using 2400 hour system	TIME <div style="border: 1px solid black; width: 60px; height: 20px; margin: 0 auto;"></div>	
WAVE PERIOD Record the time in seconds for eleven (11) wave crests to pass a stationary point. If calm record 0. <div style="border: 1px solid black; width: 60px; height: 20px; float: right;"></div>			WAVE HEIGHT Record the best estimate of the average wave height to the nearest tenth of a foot. <div style="border: 1px solid black; width: 60px; height: 20px; float: right;"></div>			
WAVE ANGLE AT BREAKING Record to the nearest degree the direction the waves are coming from using the protractor. 0 if calm. <div style="border: 1px solid black; width: 60px; height: 20px; float: right;"></div>			WAVE TYPE 0 - Calm 3 - Surging 1 - Spilling 4 - Spill/Plunge 2 - Plunging <div style="border: 1px solid black; width: 60px; height: 20px; float: right;"></div>			
WAVE LENGTH Estimate in feet the average distance between wave crests. 0 if calm. <div style="border: 1px solid black; width: 60px; height: 20px; float: right;"></div>			WIDTH OF SURF ZONE Estimate in feet the distance from shore to breakers. 0 if calm. <div style="border: 1px solid black; width: 60px; height: 20px; float: right;"></div>			
LONGSHORE CURRENT CURRENT SPEED Measure in feet the distance the dye patch is observed to move during a one (1) minute period; if no movement record 0. <div style="border: 1px solid black; width: 60px; height: 20px; float: right;"></div>			DYE Estimate distance in feet from shoreline to point of dye injection. <div style="border: 1px solid black; width: 60px; height: 20px; float: right;"></div> CURRENT DIRECTION <div style="border: 1px solid black; width: 60px; height: 20px; float: right;"></div> 0 No longshore movement +1 Dye moved toward right -1 Dye moved toward left			
PLEASE PRINT <div style="border-bottom: 1px solid black; margin-bottom: 5px; display: flex; justify-content: space-between;"> SITE NAME OBSERVER </div> REMARKS: <div style="border-bottom: 1px solid black; margin-bottom: 5px;"></div> <div style="border-bottom: 1px solid black; margin-bottom: 5px;"></div> <div style="border-bottom: 1px solid black; margin-bottom: 5px;"></div> <div style="border-bottom: 1px solid black; margin-bottom: 5px;"></div> <div style="border-bottom: 1px solid black; margin-bottom: 5px;"></div>						

Littoral Observation Report
ONR Form 32-300 (9-78)

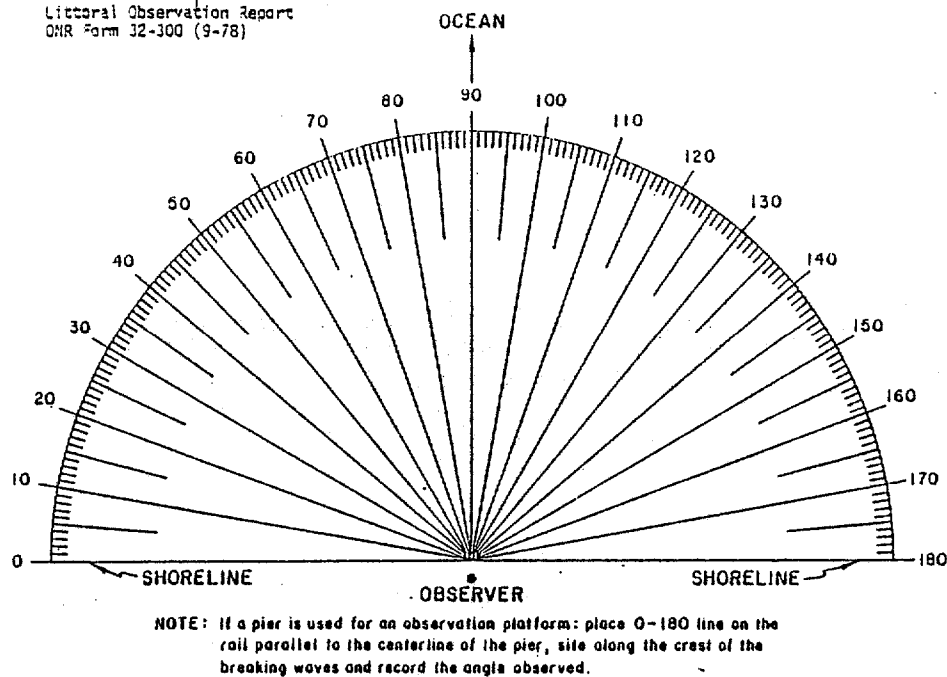


Figure 2. Modified LEO form of the type used during field experiments (recording format appears on the front of the form, wave angle protractor on the back).

measured using a calibrated staff, the base of which was fitted with a foot to prevent the staff from settling into the sandy bottom. A minimum of two individuals were required in the process. The method allowed for mobility since waves seldom broke at precisely the same point every time, but varied slightly for each consecutive shore-breaker. Two measurements were made:

1. the total height from the crest of the breaker to the bottom, H_t , and
2. the height of the trough just preceding breaking measured from the bottom, d_t , as illustrated in Figure 3. These parameters were simultaneously measured for 30 randomly selected waves, taking care to measure the information for each distinct wave train. Where more than one approaching wave train was observed, separate sets of observations were made. The average breaker height, \bar{H}_b , with variances and standard deviations were computed according to standard statistical procedure.

In addition, water level measurements seaward of breaking were made, which can be used to provide a measure of nearshore non-breaking wave activity (Figure 3) as discussed by Balsillie (1980). Thirty non-breaking wave crest and trough heights were measured and the appropriate point estimators (i.e., means, standard deviations, and variances) computed.

MOMENT WAVE HEIGHT STATISTICS

This section deals with single records or sets of nearshore wave and breaker height data. A single set of such heights provides a representation of conditions of a prevailing wave climatology at a particular locality (i.e., to account for characteristic bottom conditions) for a period of time necessary to successfully record an accurate wave height, represented by either point estimators or a probability density function, for that climatology. Such a record provides what shall be termed here, as the moment wave height or instantaneous wave height record. For instance,

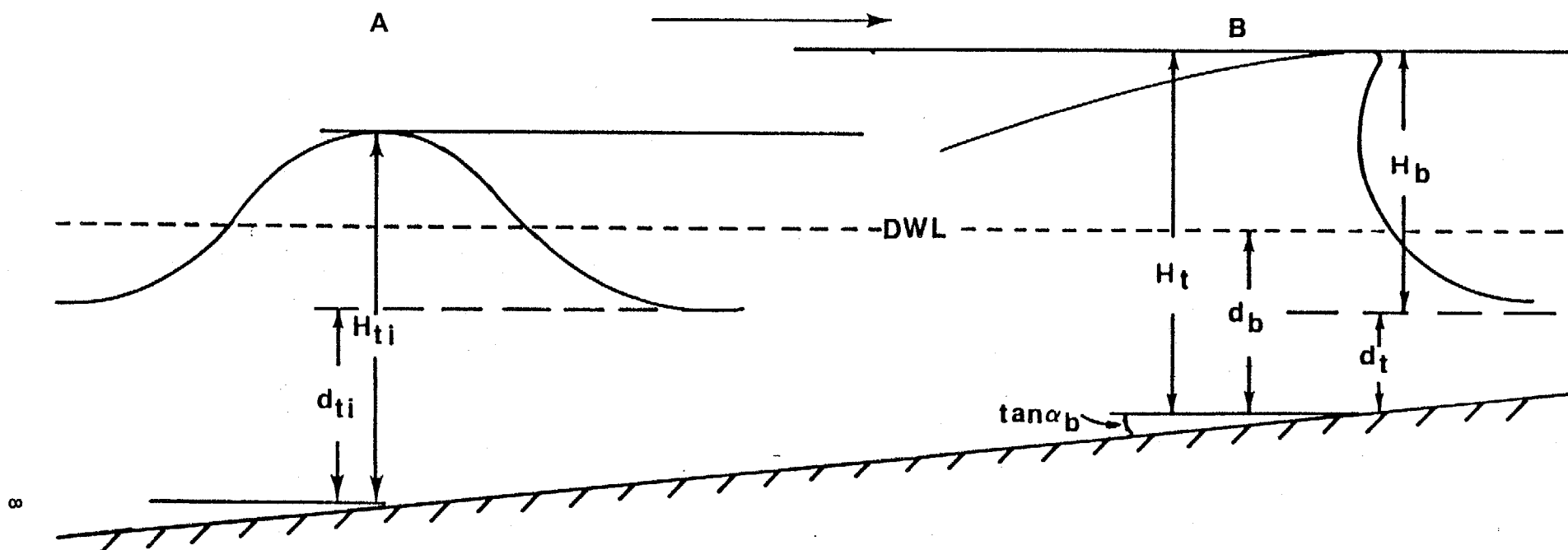


Figure 3. Nearshore and shore-breaking wave parameters; position A illustrates parameters for nearshore waves seaward of shore-breaking, position B at shore-breaking for a plunging-type breaker.

a visual estimation of the shore-breaker height (i.e., a LEO recording), a continuous 7- to 17-minute gage record represented by point estimators, or physically measured nearshore waves and breaker heights described in the previous section, are examples of such records.

Natural Wave Height Variability

Munk (1944) reports ".....wherever three consecutive waves have been recorded their heights have differed by more than 10 per cent, and whenever waves have been recorded continuously during a time interval of two minutes or more, the highest waves are usually twice as high as the lowest."

The variability of wave heights within a moment wave height record has been investigated in detail. Here, we shall look at two types of moment wave height records: 1. those where a spectra is recorded, and 2. those where heights from a single wave train are recorded.

Spectral Records

Where the local depth of water is significant a continuously recording gage can measure characteristics of many wave trains which encounter the device. For these conditions, the Shore Protection Manual (U.S. Army, 1977, Chapter 3.22) suggest that the local moment wave height measure termed the average wave height \bar{H} , can be related to the following moment wave height statistical measures:

$$\bar{H}_{rms} = 1.13 \bar{H} \quad (1)$$

where H_{rms} , termed the root-mean-square wave height, is defined by:

$$\bar{H}_{rms} = \sqrt{\frac{1}{n} \sum_{i=1}^n H_i^2} \quad (2)$$

$$\overline{H}_s = 1.6 \overline{H} \quad (3)$$

where H_s is by definition, the average of the highest 30% of the wave height of the record and termed the significant wave height.

$$\overline{H}_{10} = 2.03 \overline{H} \quad (4)$$

where H_{10} is the average of the highest 10% of wave heights of the record, and

$$\overline{H}_1 = 2.67 \overline{H} \quad (5)$$

where H_1 is the average of the highest 1% of wave heights of the record.

Kinsman (1965) showed that the average energy of a wave train is proportional to the average value of the time-related water surface elevation above the still water level, $[\eta(t)]^2$, which is identical to s^2 where s is the standard deviation of the wave record, or:

$$s = 0.5 \sum_{i=1}^n a_i^2 \quad (6)$$

where a is the wave amplitude. "Experimental results and calculations based on the Rayleigh distribution function show that the significant wave height is approximately equivalent to $4 s$ (U.S. Army, 1977, chapter 3.23). Hence, from equation (3) the average wave height, \overline{H} , for a relatively non-deformed wave seaward of shore-breaking and s , the standard deviation of the moment record, can be related by:

$$s = 0.25 \overline{H}_s = 0.4 \overline{H} \quad (7)$$

Equations (1) through (6) are plotted in Figure 4 over tropical storm and hurricane data analyzed by Goodnight and Russell (1963) which were measured by instrumentation located in 10.03 m of water, 2.41 km offshore of Burrwood, Louisiana.

Single Wave Train Records at Shore-Breaking

Moment wave height statistics of the previous section deal with a spectra of wave conditions (i.e., multiple wave trains) that may exist in a relatively significant water depth where a recording wave gage is commonly located (see Table 2). However, where shore-breaking occurs, the same moment wave height statistical constraints cannot apply.

By way of illustration, assume that the characteristics of a particular wave train approaching the shoreline are constant. Now the McCowan (1894) relationship as further studied by Weishar (1978), Balsillie (in manuscript), etc., may be applied. This relationship specifies, assuming interaction between the local wave steepness and changes in the bottom slope do not introduce complications, that the height of the wave at the shore-breaking position may be related to the water depth at that position according to $\bar{d}_b = 1.28 \bar{H}_b$ where \bar{d}_b is the average water depth and \bar{H}_b is the average shore-breaking wave height, both representing moment statistics. For example, suppose that at a particular locality three distinct wave trains are shore-incident to result in shore-breaker heights where $\bar{H}_{b1} = 0.25\text{m}$, $\bar{H}_{b2} = 0.50\text{ m}$ and $\bar{H}_{b3} = 1.00\text{ m}$ for each of the wave trains. Hence, \bar{H}_{b1} should break in a water depth of $\bar{d}_{b1} = 1.28(0.25) = 0.32\text{ m}$, \bar{H}_{b2} where $\bar{d}_{b2} = 1.28(0.50) = 0.64\text{ m}$ and \bar{H}_{b3} where $\bar{d}_{b3} = 1.28(1.00) = 1.28\text{ m}$

It becomes quite clear that a particular nearshore wave train results in moment shore-breaking wave height statistics that, like recording wave gages, are fixed in location for a particular shore-breaker episode since the shore-breaker height is depth controlled (note: wave interference

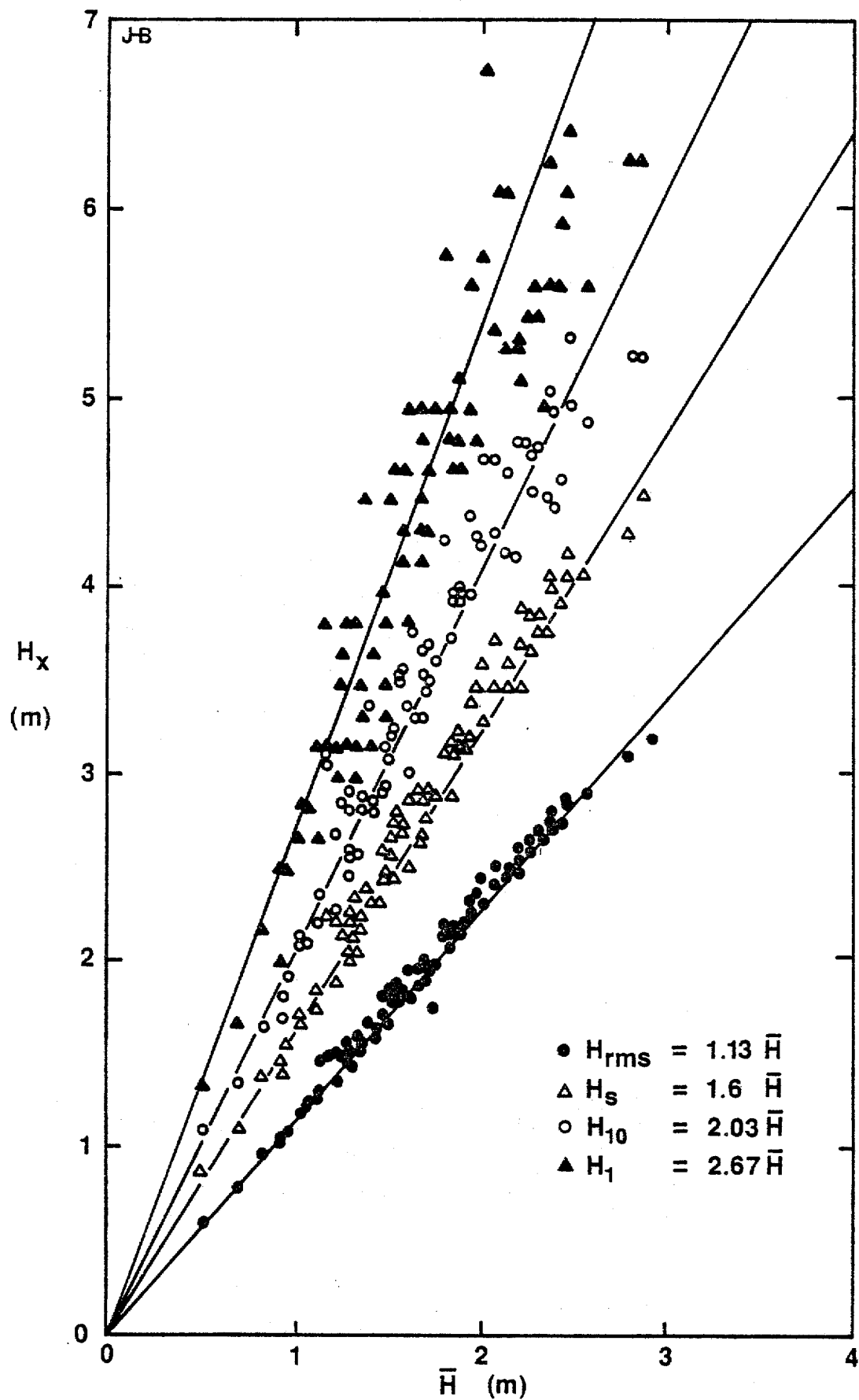


Figure 4. Moment wave height statistical equations (1) through (5) applied to Gulf of Mexico tropical storm and hurricane wave data of Goodnight and Russell (1963).

Table 2. Water depths commonly found at wave gage measurement sites (from Thompson, 1977).

Gage Location	Gage Type	Gage Range ¹ (m NGVD)	Gage ¹ Elev. (m NGVD)
EAST COAST			
Buzzards Bay, MA	Staff and Pressure	-2.4 to +11.3 (-8 to +37)	19.2 (63)
Atlantic City, NJ	Staff	-2.4 to +5.2 (-8 to +17)	5.2 (17)
Virginia Beach, VA	Staff	----- -----	6.1 (20)
Nags Head, NC	Staff	-2.4 to +5.2 (-8 to +17)	5.2 (17)
Wrightsville Beach, NC	Staff	-2.4 to +5.2 (-8 to +17)	5.2 (17)
Holden Beach, NC	Staff	-1.8 to +5.8 (-6 to +19)	4.6 (15)
Savannah, GA	Staff	-4.6 to +6.1 (-15 to +20)	15.8 (52)
Daytona, FL	Pressure	-2.1 to +5.5 (-7 to +18)	3.4 (11)
Palm Beach, FL	Staff	----- -----	4.9 (16)
Lake Worth, FL	Staff	-1.5 to +4.6 (-5 to +15)	5.5 (18)
GULF COAST			
Naples, FL	Staff	-1.8 to +2.7 (-6 to +9)	5.5 (18)
Destin, FL	Staff	-2.4 to 4.6 (-8 to +15)	3.4 (11)
Galveston, TX	Staff	-2.4 to +5.2 (-8 to +17)	5.2 (17)
WEST COAST			
Pt. Conception, CA	Staff	-3.7 to +5.5 (-12 to +18)	30.5 (100)
Port Hueneme, CA	Staff	-3.0 to +4.6 (-10 to +15)	7.0 (23)
Pt. Mugu, CA	Pressure	-3.4 to +5.8 (-11 to +19)	9.4 (31)
Venice, CA	Staff	-3.4 to +4.3 (-11 to +14)	6.0 (20)
Huntington Beach, CA	Staff	-4.0 to +3.7 (-13 to +12)	9.1 (30)

1

Original data in parentheses are in feet.

which may introduce complications is addressed later). One would not, therefore, expect that spectral moment wave height statistics apply to moment shore-breaking height statistics.

Data collected by the authors include measured wave heights at shore-breaking, to yield the following moment shore-breaker statistical relationships:

$$\overline{H}_{brms} = 1.02 \overline{H}_b \quad (8)$$

where the subscript b refers to the wave height at shore-breaking,

$$\overline{H}_{bs} = 1.23 \overline{H}_b \quad (9)$$

$$\overline{H}_{b10} = 1.37 \overline{H}_b \quad (10)$$

and

$$\overline{H}_{b1} = 1.57 \overline{H}_b \quad (11)$$

Equations (8) through (11) are plotted in Figure 5 as fitted to the field data of this study using regression techniques. The relating coefficient for equation (11) has not been fixed with certainty. However, because of the importance of equation (11) in design work, an approximation based on similitude with non-breaking equations presented earlier, Figure 6 yields a value of about 1.57.

It has been determined (Balsillie, in manuscript) that at the shore-breaking position 84% of the wave crest height lies above the SWL. Therefore, unlike the standard deviation, s , for deeper water relatively non-

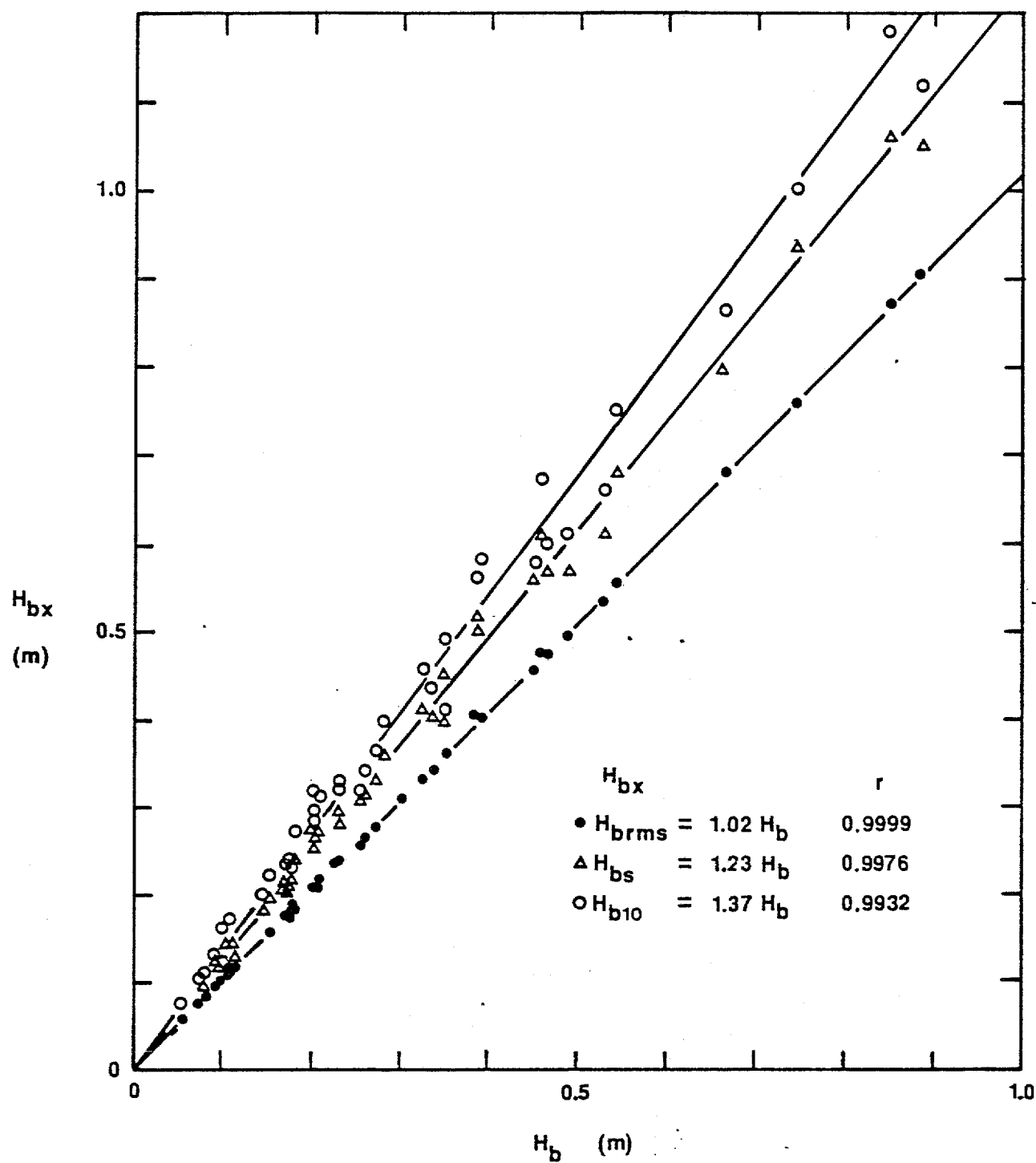


Figure 5. Moment wave height statistical equations derived for shore-breaking wave height data (single wave trains).

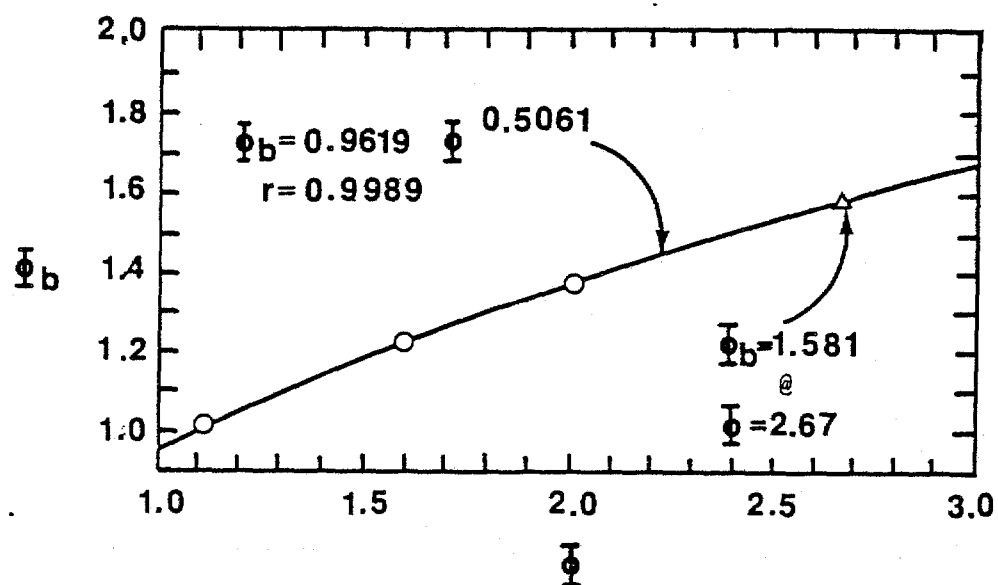


Figure 6. Relationship between the relating coefficient for shore-breaking waves (single wave trains), $\bar{\Phi}_b$, and the relating coefficient for non-breaking waves (spectral records), $\bar{\Phi}$.

deformed wave height records suitable for equation (7), the sine wave assumption cannot apply at shore-breaking and the wave amplitude is improper to use in the calculation of the shore-breaking standard deviation, s_b . In this work, the standard statistical relationship is used, such that:

$$s_b = \frac{\sum_{i=1}^n (H_b - \bar{H}_b)^2}{n - 1} \quad (12)$$

Resulting data suggest apparent simplified relationships, illustrated in Figure 7, that may be given as:

$$s_b = 0.21 \bar{H}_b = 0.17 \bar{H}_{bs} \quad (13)$$

As discussed earlier, the difference between equations (1) through (7) and equations (8) through (13) undoubtedly occurs because the former represent the total wave spectra, while the latter represent a single wave train, as provided in the following explanation. During field experiments, the authors measured highs and lows of the water surface seaward of the shore-breaking position in order to obtain the still water level. These measurements which represent the relatively non-deformed waves seaward of shore-breaking (Balsillie, 1980), include all highs (i.e., wave crests) and lows (i.e., wave troughs) and not just measurements for a single wave train. Hence, one would expect to see values which relate, for example \bar{H} and \bar{H}_s between 1.6 and 1.23 as suggested by equations (3) and (9). In fact, this is just what is seen in Figure 8, with an average relationship given by:

$$\bar{H}_s = 1.39 \bar{H} \quad (14)$$

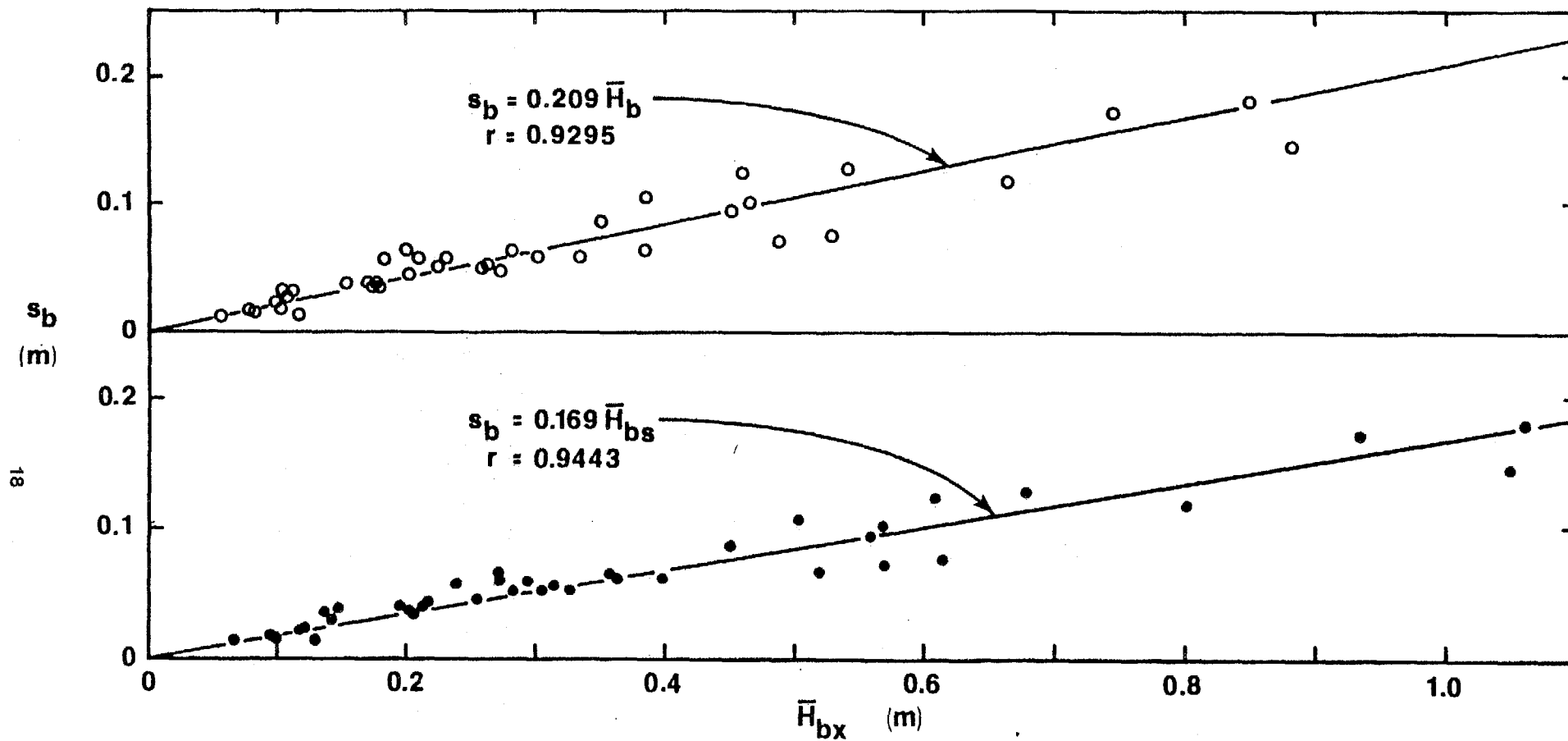


Figure 7. Relationship between the standard deviation, s_b , of the moment record and the wave height statistical parameter at shore-breaking.

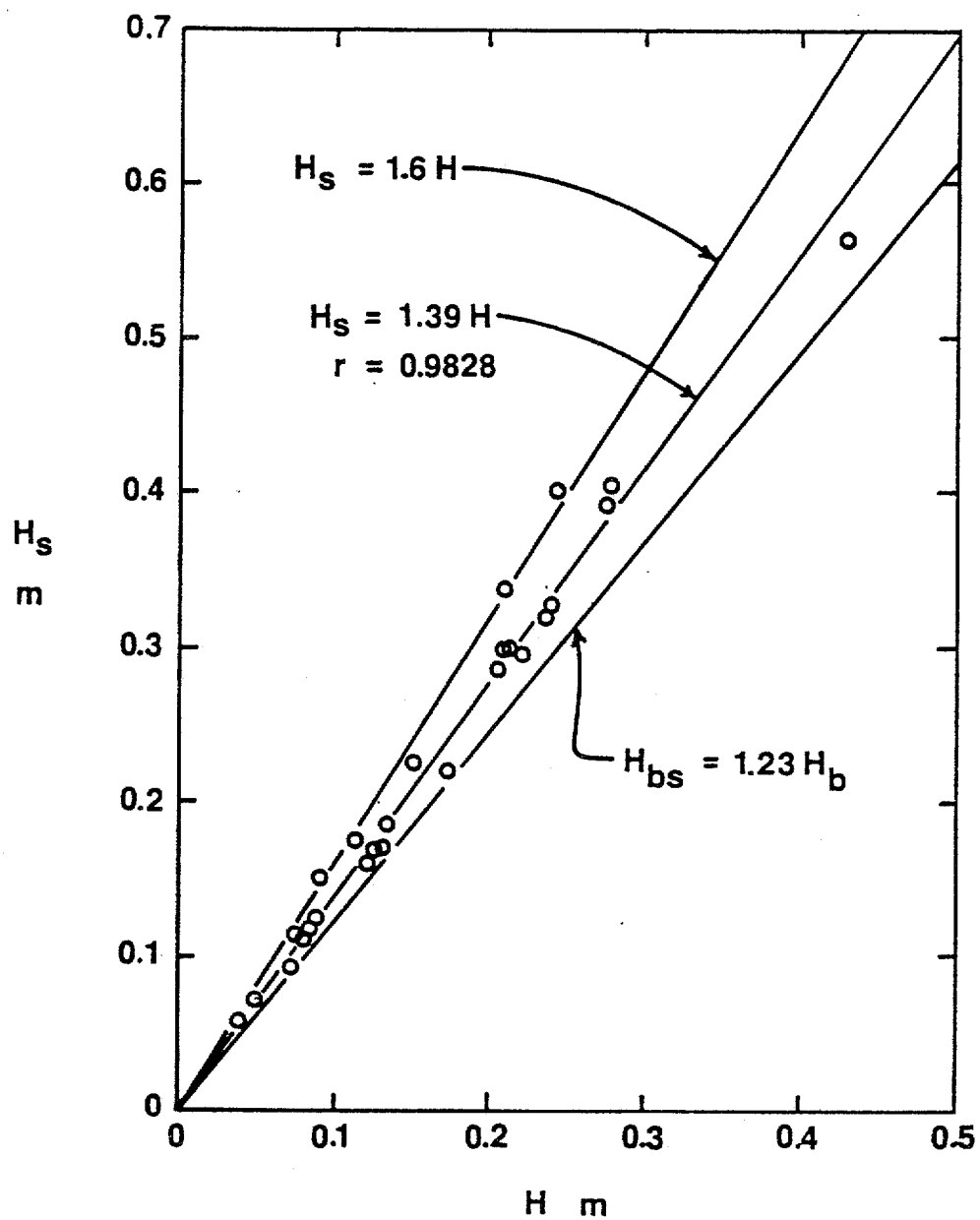


Figure 8. Relationship between \bar{H}_s and \bar{H} moment wave heights for waves seaward of the shore-breaking point.

The occurrence of secondary wave trains interfering with the shore-breaking wave train deserves attention. Balsillie (1980, in manuscripts) investigated wave transformation during shore-breaking, termed alpha wave peaking, and found the complex non-linear processes, during which the waves become critically distorted in profile view, to be dependent on the wave steepness and depth conditions. However, secondary wave trains which may interfere with the shore-breaking wave train are not subject to the same alpha peaking constraints, since these smaller waves are as yet in relatively deeper water and, hence, are usually less distorted. Secondary waves, therefore, would not be expected to contribute to the moment statistical distribution at shore-breaking to the extent that is possible offshore in relatively deeper water where all the waves are, by comparison, less distorted.

It is known that at any one time at a particular nearshore locality, several to many wave trains are usually present. For the wide range of localities and random wave conditions representing this study, even though only the most prominent wave trains were observed and then measured in the field, it is deemed reasonable to assume that any such interference from secondary wave trains has been included in the results presented. The excellent agreement exhibited in Figure 6 suggest that equations (8) through (12) are the proper relationships to apply to shore-breaking wave conditions.

Relationship between Spectral and Single Wave Train Moment Statistics

The relationship between the coefficient for determination of spectral moment statistics, Φ , and that for single wave train moment statistics at shore-breaking, Φ_b , as illustrated in Figure 6, may be given by:

$$\Phi_b = 0.96 \sqrt{\Phi} \quad (15)$$

where the continuum of Φ values appears to be given by:

$$\Phi = 1.0 + 2.8 (P - 0.5) + 13.33 (P - 0.5)^2 - 83.2 (P - 0.5)^3 + 119.5 (P - 0.5)^4 \quad \left\| \begin{array}{l} 0.5 < P < 1.0 \end{array} \right. \quad (16)$$

and illustrated in Figure 9. From the previous two equations it is interesting to note that:

$$\bar{H}_{rms} = \bar{H}_{46} \quad (17)$$

for the total spectra rather than equations (1) and (2), and:

$$\bar{H}_{brms} = \bar{H}_{b46} \quad (18)$$

in lieu of equation (8).

The choice of which to apply, i.e., Φ or Φ_b , for a particular locality and design solution(s) would not be problematic if it were not for the significantly large difference between Φ and Φ_b , ranging from 9.7% between \bar{H}_{rms} and \bar{H}_{brms} to as much as 40.2% between \bar{H}_1 and \bar{H}_{b1} .

In coastal engineering applications it may be more responsible to use moment statistics, such as those suggested by the Shore Protection Manual (U.S. Army, 1977, Chapter 7.1) which rather than representing the total spectra represent single wave train shore-breakers. For

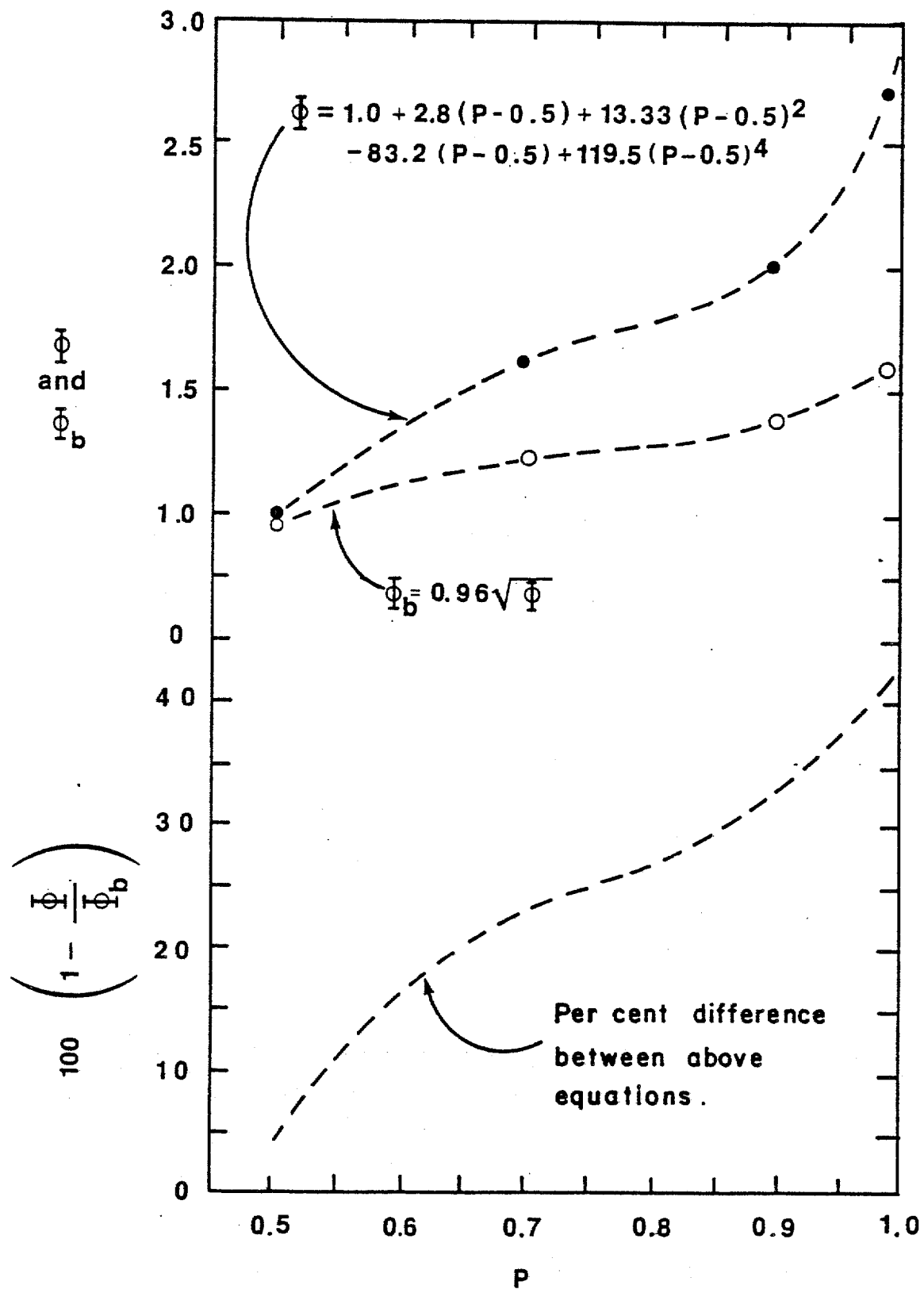


Figure 9. Relationship between ϕ and ϕ_b .

instance, where design of structures such as a pier, offshore detached breakwater, an offshore tethered device, etc. is the goal then the total wave spectra, given by equations (1) through (7), may be the better design choice. However, where the structure is determined to be located in the surf zone during a selected design storm event, or impacted as the result of dynamic setup, runup, and erosion (both horizontal and vertical) from final shore-breaking wave activity the single wave train approach may be more applicable.

A specific example of the application of the two types of moment wave height statistics may be illustrated by considering longshore transport prediction; some background of which is first required.

The presently accepted general form of the equation (Longuet-Higgins, 1970, 1982; Komar, 1969, 1971; U.S. Army, 1977; etc.) for prediction of the instantaneous longshore transport, Q , is given by:

$$Q = k \frac{\frac{\rho_f g}{8} H_{b\alpha}^2 c_g (\sin \theta_b) \cos \theta_b}{g(\rho_s - \rho_f)a'} \quad (19)$$

where θ_b is the angle in degrees of wave approach to the shoreline at shore-breaking, c_g is the shallow water group wave speed, ρ_f is the fluid mass density, ρ_s is the sediment mass density, g is the acceleration of gravity and a' is the percent of void space in the sediment.

Where the longshore current is known, Balsillie (1977a) has shown that equation (15) becomes:

$$Q = k' \frac{\frac{2 \rho_f g}{5 \pi} H_{b\alpha} c_f \frac{W v_m}{Z}}{g(\rho_s - \rho_f)a'} \quad (20)$$

where W is the surf zone width, v_m is the measured longshore current speed,

c_f is the bottom friction coefficient, and Z is the dimensionless shore-breaker distance across the surf zone.

Grant (1943) discussed the importance of shore-breaking wave activity in longshore transport mechanics as the means by which bottom sediment is agitated and placed in suspension, where upon existing currents induce a net transport of the agitated and suspended sediment. In fact, the dimensionless proportionality constants, k and k' , are related to the power of the shore-breaking waves. About this, Inman and Bagnold (1963, p. 546) state "If the whole of the power in the breaking wave is dissipated between the plunge line and the shore, then..... $[(\rho_f g/8)H_b^2 c_g]$ would be the power available to move sediment over the entire width of the surf zone. In fact, however, a high proportion of the power dissipated in the surf zone is dissipated by means other than bottom friction,, and thus the factor k [and, therefore, k'] is an index of the proportion of power dissipated in moving sediment."

It is clear, therefore, that k and H_{bx} are related. In fact, the value of k is dependent on the moment wave height statistic considered. For instance, Komar (1969) specifies the shore-breaking wave height in equation (18) to be given by \bar{H}_{brms} that where at shore breaking $c = c_g = \sqrt{g d_b}$ $= 1.28 g \bar{H}_b$ then $k = 0.77$. On the other hand, the Shore Protection Manual (U.S. Army, 1977) considers the shore-breaking wave height in equation (18) to be given by \bar{H}_{bs} , and $k = 0.39$ where $c = c_g = \sqrt{2 g \bar{H}_b}$.

An additional factor, expressed as a direct function of \bar{H}_b , affecting the value of k is the wave speed at shore-breaking. Recently, however, Balsillie (in manuscript) has determined that $c_b = c = c_g = \sqrt{1.6 g \bar{H}_b}$. Now, Komar's k for \bar{H}_{brms} becomes 0.69 and k for \bar{H}_{bs} becomes 0.34.

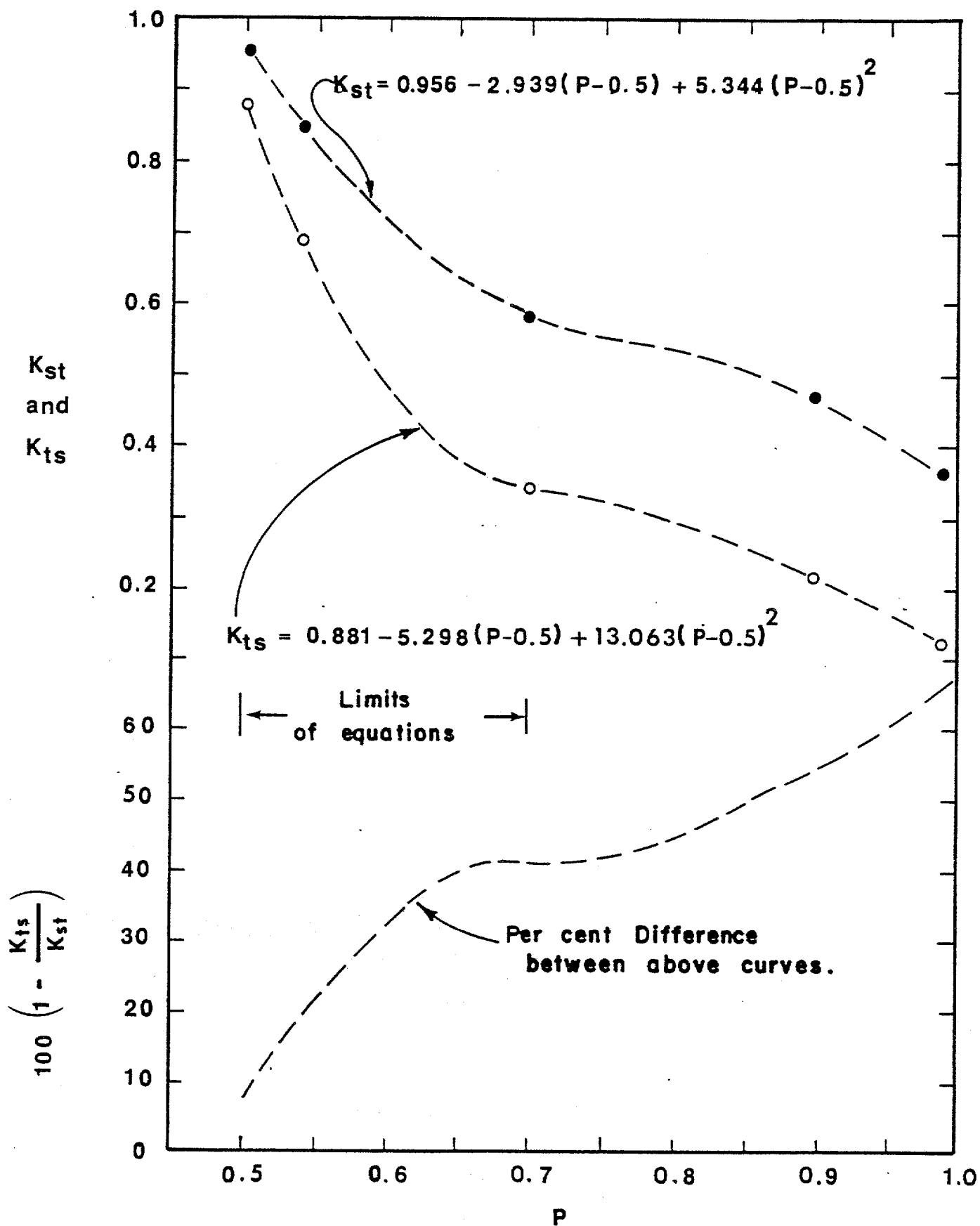


Figure 10. Dimensionless longshore transport proportionality constants for the total spectrum, k_{ts} , and for the single wave train at shore-breaking, k_{st} , for equation (19).

be represented (Figure 11) by:

$$k'_{ts} = 0.59 - 1.605 (P - 0.5) + 3.25 (P - 0.5)^2 \quad \left\{ \begin{array}{l} 0.5 < P < 0.7 \\ \text{or} \\ 30 < \alpha < 50 \end{array} \right. \quad (23)$$

for the total spectra, and by:

$$k'_{st} = 0.53 - 0.824 (P - 0.5) + 1.219 (P - 0.5)^2 \quad \left\{ \begin{array}{l} 0.5 < P < 0.7 \\ \text{or} \\ 30 < \alpha < 50 \end{array} \right. \quad (24)$$

for a single wave train at shore-breaking.

Mathematical representation of the entire length of the curves given in Figures 10 and 11 would be somewhat more complex than is suggested by equations (21) through (24). However, since in the literature k values have been specified only for moment wave height statistics ranging from the average to the significant wave height, equations (21) through (24) would appear to be adequate.

The purpose of the preceding exercise is not an attempt to determine precision k and k' values. Rather, based on available information the intention is to illustrate the potential magnitude of differences between k values which are apparently associated with total spectra statistics and single wave train shore-breaking statistics. The per cent difference between results of the two types of k -values, i.e.,

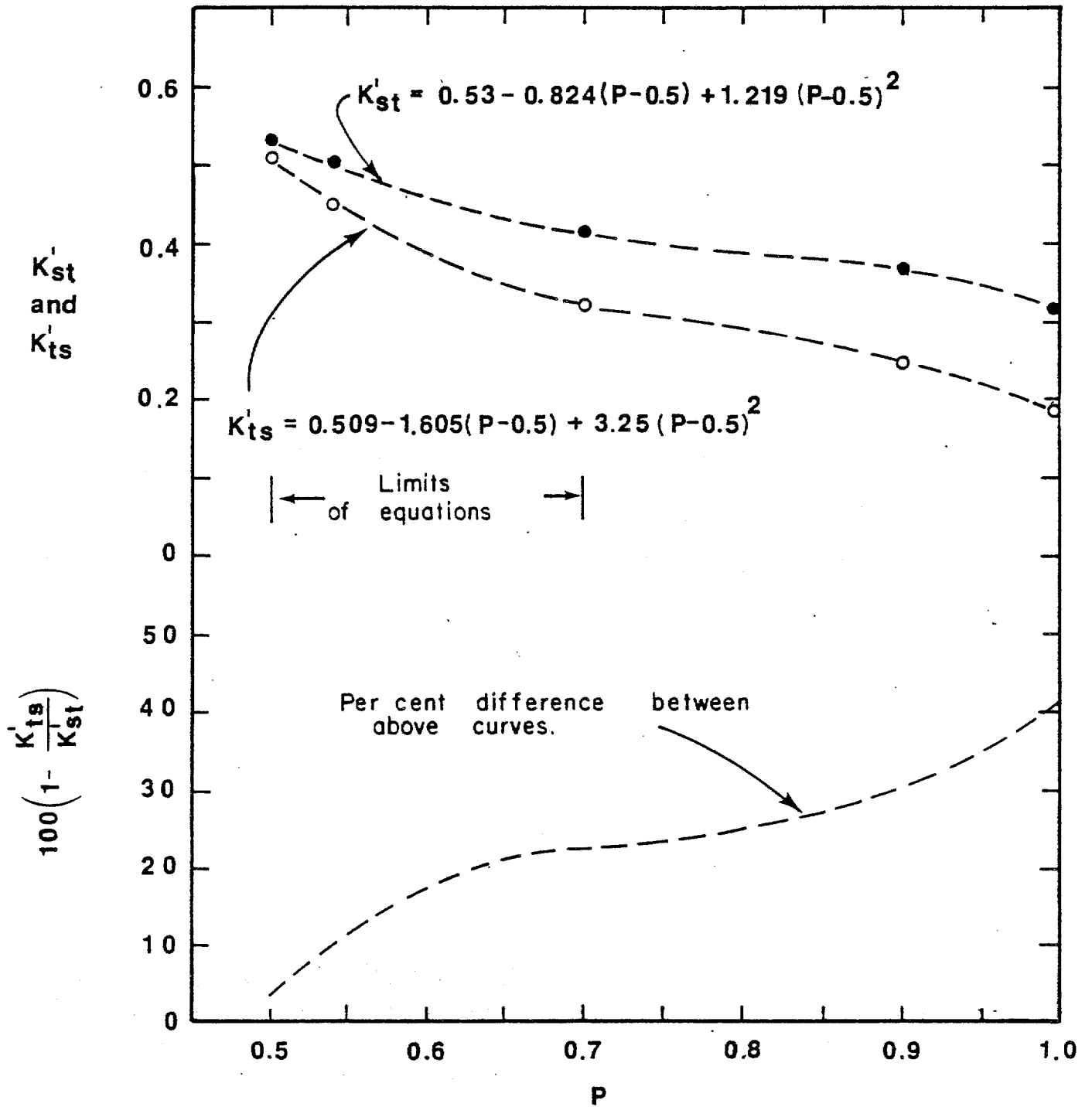


Figure 11. Dimensionless longshore transport proportionality constants for the total spectrum, K'_{ts} , and for the single wave train at shore-breaking, K'_{st} , for equation (20).

k_{ts} and k_{st} for equation (19) and k'_{ts} and k'_{st} for equation (20), though greater for equation (19) as illustrated in Figures 10 and 11, may in both cases be assessed as significant. For instance, where a single train of shore-breakers are present, such as in a laboratory wave basin study, moment statistics given by equations (8) through (13) and k_{st} and k'_{st} factors would appear to constitute the applicable data. In fact, where nearshore, non-shore-breaking spectral records are known then record wave components could be transformed to shore-breaking and the appropriate single wave train moment statistics applied to each shore-breaker episode.

Over-Estimation of Visual Observation

The over-estimation of wave heights using visual techniques has been reported to occur by Munk (1944) wherein he made recommendations for "..... observing and reporting wave and breaker characteristics." He found (U.S. Army, 1977, p. 3-2) that when the wave height was estimated by an experienced observer the result corresponds to the average of the highest one-third of the measured wave record (reported as the average of the highest 30% in Munk's report) and termed the significant wave height.

Following from the above, it becomes important to inspect for over-estimation for both inexperienced (i.e., I group) and experienced (i.e., E group) observer data. Cross-plots of the measured breaker height, \bar{H}_b , and the simultaneously observed breaker height, H_{bLE0} , are provided in Figures 12 and 13 for the I and E groups, respectively.

Following Munk's (1944) analytical approach, the average value of the ratio H_{bLE0} / \bar{H}_b is used to indicate the degree of over-estimation. For the I group:

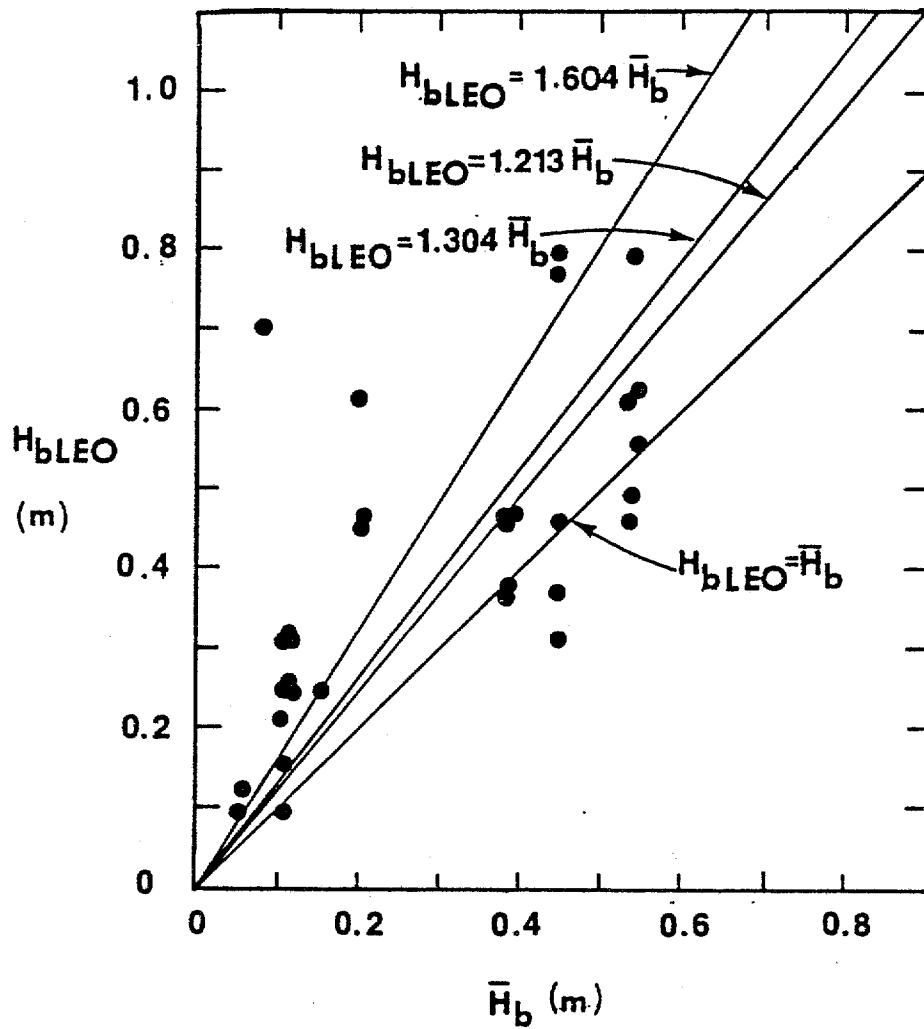


Figure 12. Plot of measured average shore-breaker heights, \bar{H}_b versus observed shore-breaker heights, H_{bLEO} , for inexperienced (i.e., I group) observers.

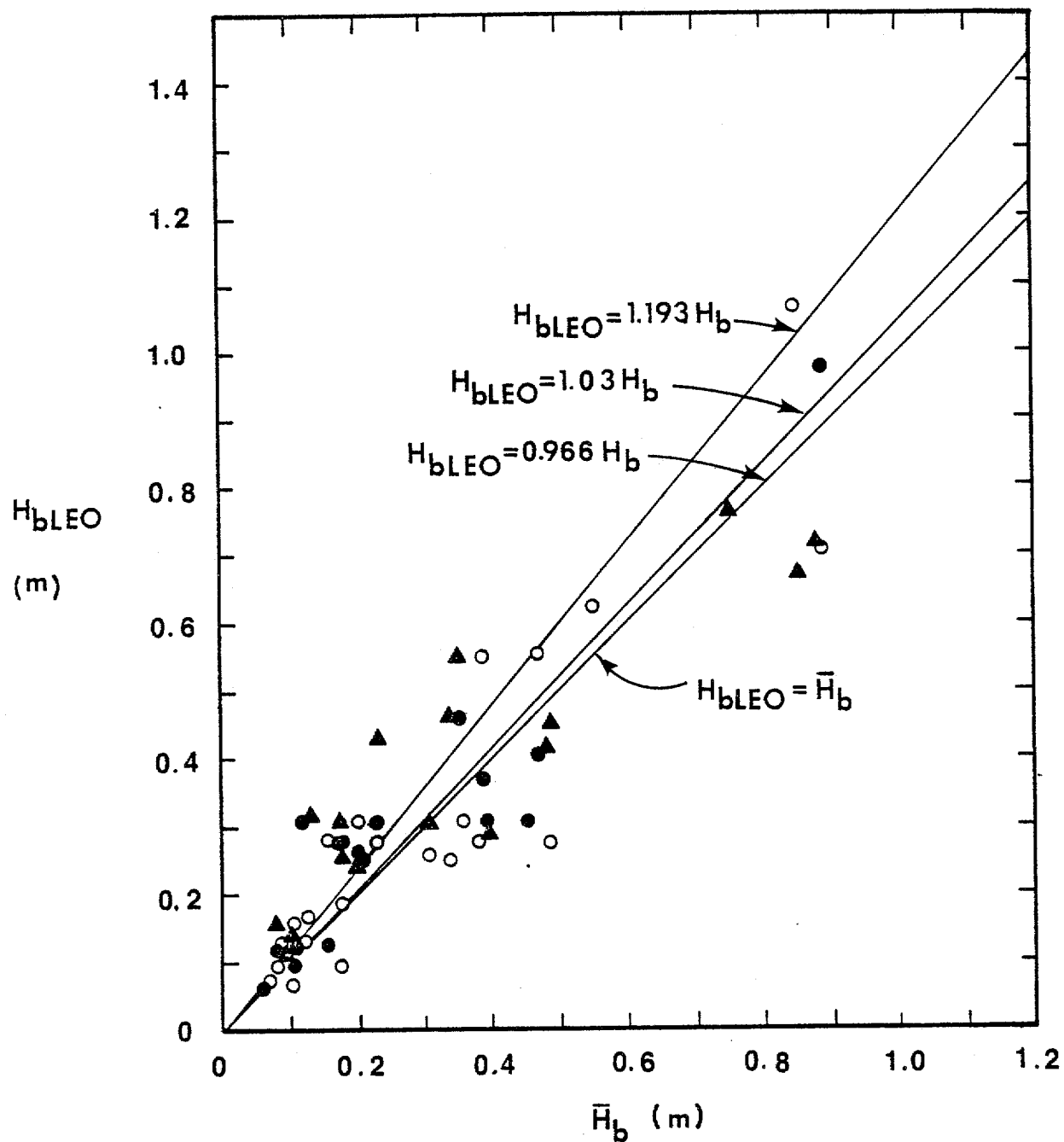


Figure 13. Plot of measured average shore-breaker heights, \bar{H}_b , versus observed shore-breaker heights, H_{bLEO} , for experienced (i.e., E group) observers.

$$H_{bLE0} = 1.604 \bar{H}_b \quad (25)$$

which is in agreement with equation (3), and

$$H_{bLE0} = 1.193 \bar{H}_b \quad (26)$$

for the E group, which is more in agreement with equation (9). The difference between equations (25) and (26), which according to a Student's t test are significantly different to at least the 95% confidence level, illustrates that experienced observers report results closer to actual wave heights, while inexperienced observers tend to over-estimate.

An alternate approach to the above is to fit approximations to the data of Figures 12 and 13 using linear regression techniques. Two types of regression models are used. The first, a predictive regression, is the regression of X on Y. However, since it would seem appropriate that the fitted line would pass through the origin of the cross-plotted data, the method of Krumbein and Graybill (1965, p. 240) is employed to yield:

$$H_{bLE0} = 1.213 \bar{H}_b \quad (27)$$

for the I group where the product-moment correlation coefficient, r, is 0.9309 and the approximate 95% confidence limits for the slope are 1.127 and 1.300. For the E group:

$$H_{bLE0} = 0.966 \bar{H}_b \quad (28)$$

where $r = 0.9656$ and the 95% confidence limits for the relating coefficient are 0.892 and 1.098.

The second type of regression is the functional regression which

provides a measure of the central trend of the natural distribution (Ricker, 1973, p. 412). Again, forcing the line through the origin, this method yields:

$$H_{bLEO} = 1.304 \bar{H}_b \quad (29)$$

for the I group where $r = 0.9309$ and the 95% confidence limits are 1.217 and 1.391. For the E group:

$$H_{bLEO} = 1.030 \bar{H}_b \quad (30)$$

where $r = 0.9656$ and the 95% confidence limits are 0.928 and 1.134.

Again, the experienced observer group appears to provide significantly different and more realistic results than the inexperienced group. However, the difference in results between the two analytical methods poses difficulties. The first method that employed by Munk (1944) is that which is now used as a standard from which the significant wave height is defined, and yet it is the second method regression which probably provides a better representation of actual conditions.

Conceding that linear regression is the more robust method for determination of the relationship between observed and measured shore-breakers (i.e., rather than a comparison of average results as used by Munk (1944), quantified by equations (25) and (26)), it can be concluded that while inexperienced observers tend to over-estimate the average shore-breaker wave height by 21 to 30% (quantified by equations (27) and (29)), experienced observers closely report the actual average wave height at shore-breaking (quantified by equations (28) and (30)). Hence, the long-held consideration that experienced observers tend to over-estimate and report the significant wave height is not substantiated for shore-breaking waves.

Error Associated with Visual Observation

Although it is desirable that an observer making LEO reports has aids to judge the size (i.e., height) of shore-breaking wave activity, such as known dimensions of pier piling and attendant structural features or some other object, such aids are the exception. Therefore, the condition of unaided visual observation or "guesstimation" must be assumed. Even so, the accuracy of unaided observations may be enhanced by proprioceptive information available to the observer; for example the observer may be a seasoned surfer with acquired skills concerning the characteristics of waves, or a trained and experienced observer acquired under the tutelage of a persistent and consolidated LEO program.

Quantification of the error associated with unaided visual observations of shore-breaking wave heights is not a straightforwardly simple task. Prior to such an attempt, perhaps it would be of value to first discuss psychological ramifications of visual perception.

The Psychological Attribute of Size Constancy

It is a fact from the physics of optics that the retinal image of an object doubles in size whenever its distance from a stationary point of observation is halved. There is, however, a phenomenon termed size constancy which "..... is the tendency for the perceptual system to compensate for changes in the retinal image with changes of viewing distance" (Gregory, 1978). In other words, the human perceptual system tends to compensate by doubling the size of the image with each doubling in distance from the observation point (i.e., Emmert's Law). Considerable work on the subject has been accomplished for stationary objects (Thouless, 1931, 1932) and moving objects (Antis, Shopland and Gregory, 1961; Gregory and Ross, 1964a, 1964b; Gregory, 1978). Gregory (1978) reports that the brain is responsible for scaling the optical retinal image.

to proportions representing actual sizes of objects lying at various extended distances.

One must understand that size constancy is an automatic mental process. It may be likened to the ability of a person with normal reading skills he or she does not dwell upon individual letters in a word, but automatically processes the entire word or even entire phrases. An example of how the size constancy phenomenon works occurs, say, where an observer is to make consecutive reports at two relatively close LEO sites, the first with a relatively shallow bottom slope of $\tan\alpha_b = 0.02$ and second with a steeper slope of $\tan\alpha_b = 0.05$. Let us assume for simplicity that a single wave train is present and that incoming wave characteristics are not significantly different between sites to result in a 1.5 m (5-foot) plunging shore-breaker. At the first site the plunger will break 98 m (320 feet) offshore, while at the second 39 m (128 feet) from the shoreline. Even with the significant difference in viewing distance, the size constancy phenomenon will function.

There are, however, limits to the size constancy phenomenon. Following the initial work of Decartes (1637) recent psychological investigations (e.g., Gregory, 1978) note that when viewing distances become too great the phenomenon tends to malfunction. Precise knowledge of the malfunction distance is not known, but is dependent upon attendant factors related to the behavior of the object observed and the environment in which it may exist. For the littoral environment pertinent additional factors include: 1. wave speed, 2. degree of sea-state confusion, and 3. source and degree of illumination. The speed with which a wave shore-breaks may affect recognition, although here the observer has the advantage of repeated shore-breaking. Research has indicated that size constancy recognition is better for objects approaching the observer than

for those moving away, which may offer an additional advantage to shore-based wave observation. As the sea-state becomes more confused, that is, the number of wave trains increases, recognition can become more complex particularly where the surf zone becomes significantly wide. The position of the sun, degree of cloud cover, and other weather conditions can also affect the resolution of visual perception.

Despite the errors which can creep into visual observations, the phenomenon of size constancy is an attribute which needs to be recognized, and which undoubtedly contributes significantly to the reasonable magnitude of LEO shore-breaking wave height observations.

Cognitive Methodology of Height Estimation

LEO shore-breaker heights are observed and reported in units of feet (they have been converted to S.I. units in this paper, since the control data were measured in the latter units). In addition to the automatic process of size constancy, there is a conscious method that is employed in wave crest height determination. Upon viewing, the observer first determines the height to the nearest foot. Having made that decision, he can then consciously make the determination whether the height is greater or less than the selected nearest-foot determination by one-half a foot. This "halving process" may be continued and reports made to the closest one-tenth of a foot. The degree to which the halving process may be carried is dependent on the skill and confidence of the observer for the given conditions and the distance of observation. One may anticipate that "halving" is more complete for close waves, becoming less complete as the observation distance increases.

An Error Analysis

Variability associated with measured shore-breaker heights (i.e.,

control data) for a single wave train is given by equation (13). Comparison between the natural variability about the mean of the control heights and the magnitude of deviations of the observed heights from the control data can be used to gain insight as to expected experienced observer error.

It can be considered that the general distribution of the measured shore-breaker data is Gaussian, since distributions of the control data plot as straight lines on normal probability paper (Figure 14). Therefore, $\bar{H}_b \pm 1s_b$ would include 68% of the distribution, $\bar{H}_b \pm 2s_b$ 95% of the distribution, and $\bar{H}_b \pm 3s_b$ 99% of the distribution, where s_b is the sample standard deviation. Hence, a measure of the comparative variability can be given by:

$$\frac{\bar{H}_b - H_{bLEO}}{c s_b} \leq 1.0 \quad (31)$$

that, if true, indicates that the LEO estimates are within bounds of the actual expected variability exhibited by the control data, where c indicates the number of standard deviations considered about the mean. Evaluation of equation (31) shows that 44% of the LEO estimates are within ± 1 standard deviation of the control data, 66% are within ± 2 standard deviations of the control data, and 87% are within ± 3 standard deviations.

Assuming the essentially one-to-one correlation between \bar{H}_b and H_{bLEO} (e.g., equations (28) and (30)) equation (13) would appear to provide a useful measure of the observation error. The application of equation (13) is illustrated in Figure 15. By using absolute deviations (i.e., $\bar{H}_b - H_{bLEO}$) an average error, E_{avg} , was determined using regression. It was found that E_{avg} corresponds closely to equation (13) and:

$$E_{avg} = \pm 0.21 H_{bLEO} \quad (32)$$

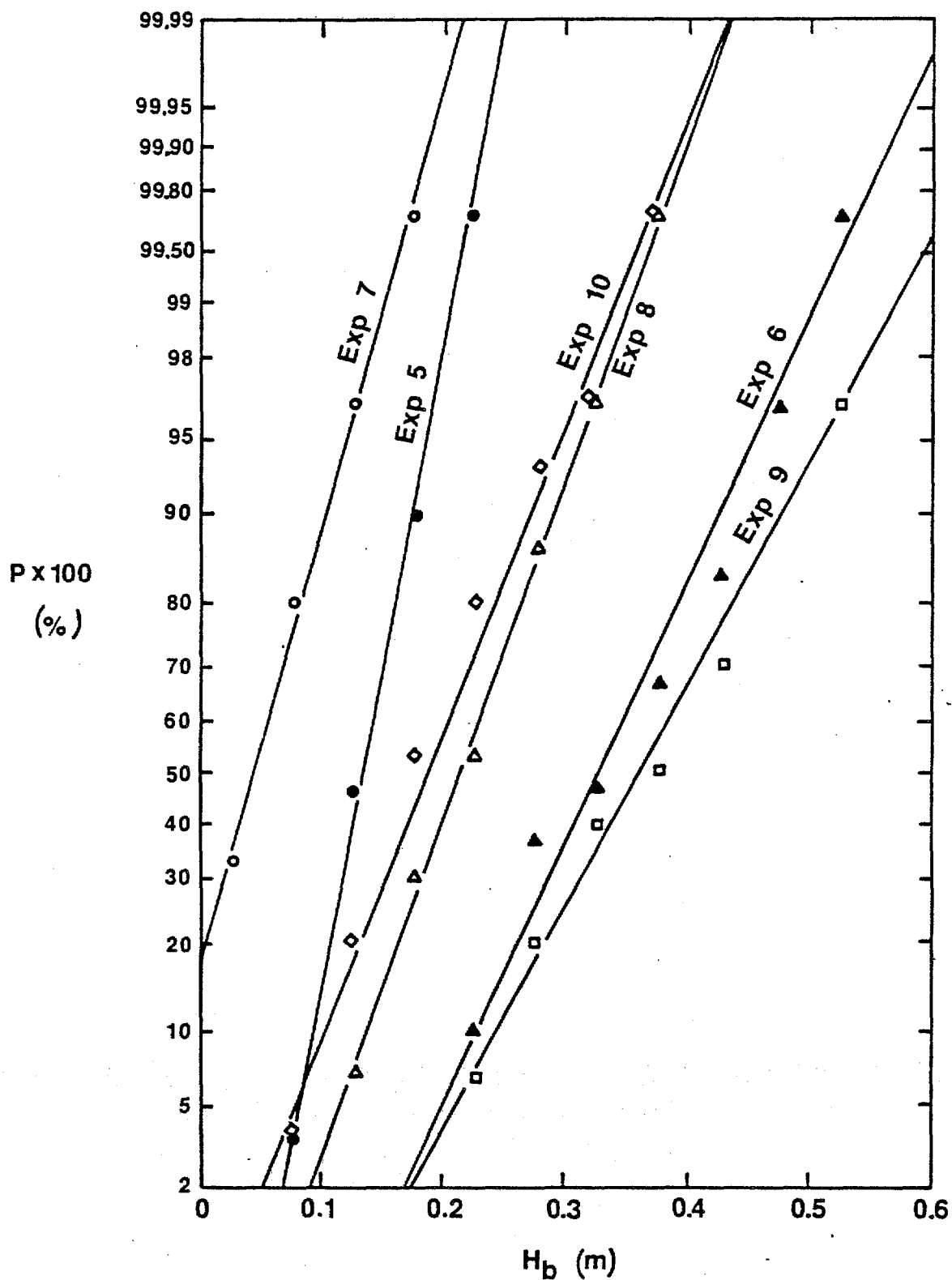


Figure 14. Typical plots of measured shore-breaker wave height data, H_b , indicating a Gaussian probability distribution.

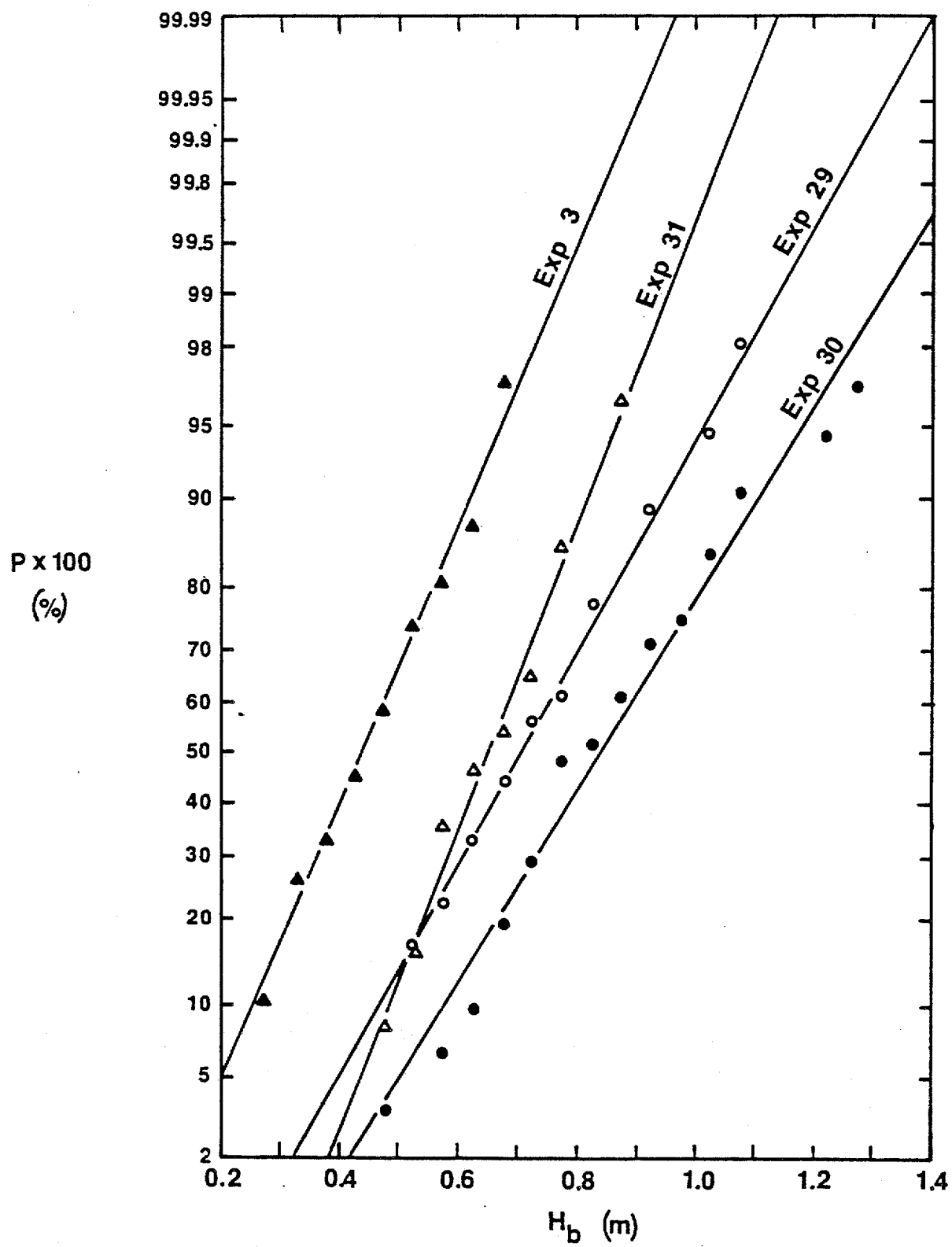


Figure 14. (cont.)

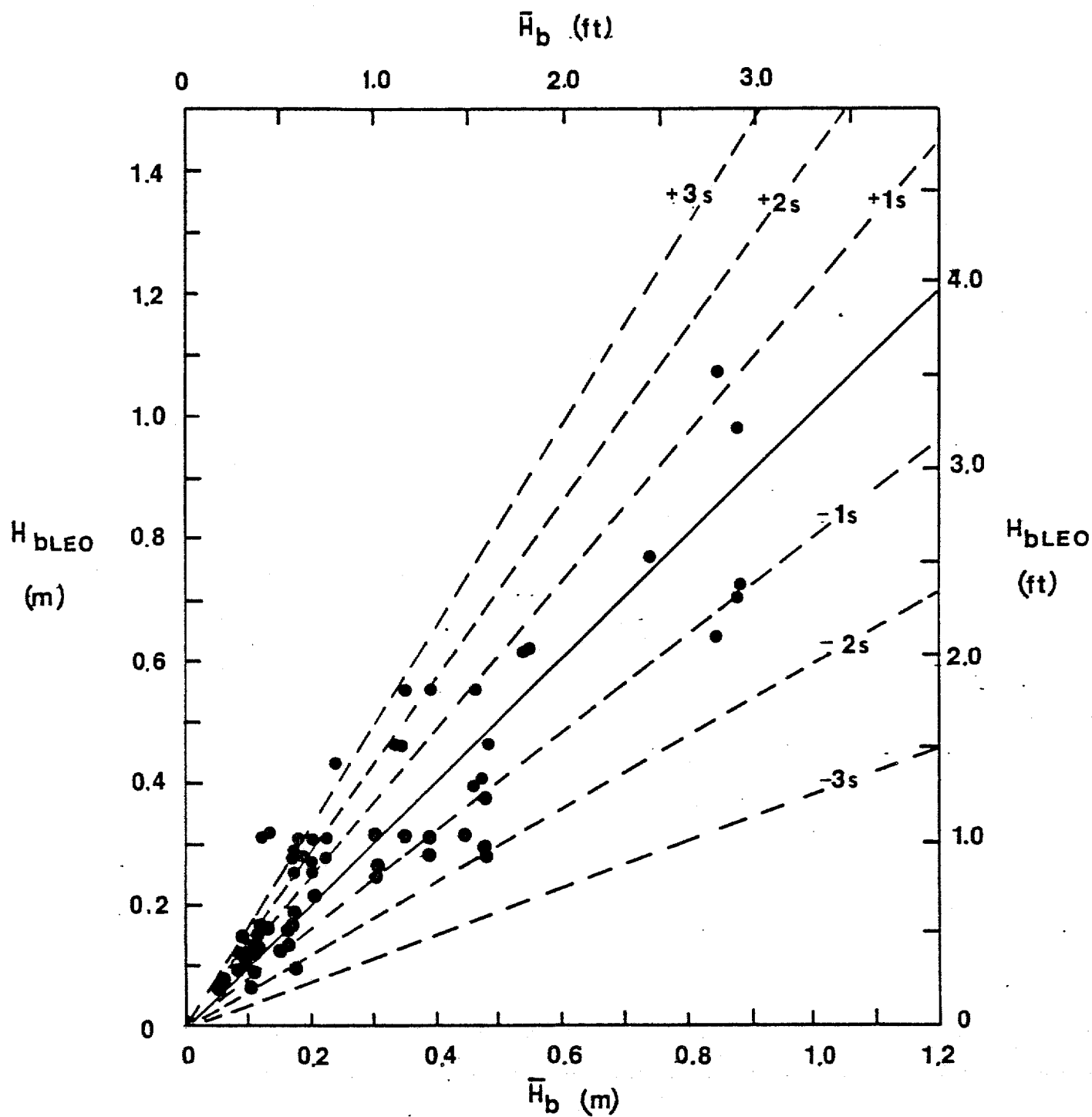


Figure 15. Plot for error analysis of Figure 13 based on the standard deviation.

may be stated. From Figure 15 a maximum error, E_{\max} , would appear to be adequately given by $\pm 3s_b$, such that:

$$E_{\max} = \pm 0.62 H_{bLEO} \quad (33)$$

Equation (32) is an optimistic result, since it is at least as good as existing wave theories in which the error is $\pm 20\%$. Equation (33) suggests a significantly larger maximum error. However, one must recognize that a single wave observation has little importance when the objective of the data collection effort is to provide long-term results and that the uncertainty of the average of a series of reports is much less than that of a single report.

LONG-TERM SHORE-BREAKER HEIGHT DISTRIBUTION AND CLIMATOLOGY

Information about the long-term distribution of sea states is essential in many coastal engineering applications. Harris (1972) states "..... analytic distribution functions are useful in organizing data, even when their precise validity is open to question", and reports that certain characteristics of waves need to be considered, specifically: 1. there are no negative values, and 2. low positive values are common and large values rare. However, for coastal engineering design purposes, it is the higher wave height values which have the greater importance and should be given relatively more weight than the lower waves.

Harris (1972) further states "in view of the unsatisfactory quality of most wave records, it appears that only the simplest of suitable distribution functions can be justified." Generally, four distribution functions..... the Rayleigh, the log-normal, the exponential, and the extremal type-I..... have been suggested (Harris, 1972; Weggel, 1971). Harris (1972) reports that while for individual waves within a single observation period (for the entire spectrum) the Rayleigh distribution provides an excellent approximation; based on experimental plots it is not, however, the best for representing

long term distributions of wave heights and Harris suggests the exponential distribution because "..... it emphasizes the relatively well known larger waves and gives little space to the less well known smaller waves."

While the Rayleigh distribution can be dismissed, the other types of density distribution functions given above were investigated using LEO data of Bruno (1971) and Balsillie (1975a, 1975b). Results indicate that none of the density distribution functions resulted in a consistent relationship. This is undoubtedly due to the presence or lack of higher shore-breakers in the record which tend to alter the shape of the curve. However, the usefulness of a particular probability density distribution representing a time series requires some knowledge and understanding of just what a data collection effort, such as the LEO program, can or cannot represent. Types of shore-breaking wave height conditions which may contribute to the density distribution of a visual data collection effort may be identified as: 1. shore-incident forced storm waves, 2. free or coasting shore-incident storm-generated waves, and 3. day-to-day, normally expected wave activity.

The first category, forced shore-incident storm waves, are seldom reported in the LEO record due to the particularly severe weather conditions which tend to discourage observation. For instance, one would not expect LEO observers to be on the beach as a hurricane makes impact at the site.

The second category, free or coasting shore-incident storm breakers, may often be included in a LEO record. These breakers resulting from waves generated by storms far out at sea (i.e., the storm does not impact the observation site), have undergone dispersion mechanics to become free or coasting waves (Mooers, 1976; Balsillie, et al., 1976) and reach the shoreline under locally non-inclement weather conditions which do not

discourage observers from making a report. These higher waves have the characteristics that they may induce an inflection point in the probability plot.

The third category, normally expected shore-breaker activity, is particularly suited to LEO data in terms of predictability from a density distribution, since the record is generally devoid of extreme values.

Forced Shore-Incident Storm Waves

As noted above, unless forced shore-incident storm wave activity is specifically noted in a visual shore-breaking wave activity report, such waves can generally be considered as non-existent in the visual time series record.

Normally Expected Shore-Breaker Activity

While higher or more extreme values in a time series tend to influence the shape of the curve of the resulting density distribution, it is the point estimators which provide cogent numerical references by delineating the nature of the central tendency of the time series distribution. One of the more problematic concerns which has faced the LEO program is how many observations are required per monthly time period to provide statistically reliable point estimators. If too few observations are made then point estimators may not provide reliable results; if too many observations are made then effectiveness of the data collection program may be over-maximized and resources wasted.

An autocorrelation analysis was conducted to determine the tendency to which a LEO shore-breaker height is independent of previously recorded breaker heights in the record. The samples, which must represent 50 or more consecutive observations, are listed in Table 3 and were selected to minimize the number of missing observations for data available to the

Table 3. Autocorrelation data and statistics for LEO shore-breaker observations.

Location	LEO Sta. No.	Time Period	No. Obs.	R _k
FLORIDA - LOWER GULF COAST				
Blind Pass (Aquaterium), St. Petersburg	---	Dec. 1978 and Jan. 1979	53	2.0
Blind Pass (N-2) " "	---	Dec. 1978 and Jan. 1979	53	2.0
FLORIDA - PANHANDLE GULF COAST				
Grayton Beach	12110	Oct. and Nov. 1969	61	2.5
" " "	"	Nov. and Dec. 1969	60	2.0
" " "	"	Dec. 1969 and Jan. 1970	66	3.0
" " "	"	Mar. and Apr. 1970	59	1.5
" " "	"	Oct., Nov., Dec. 1969	91	2.5
" " "	"	Oct., Nov., Dec. 1969 and Jan. 1970	122	2.5
J. C. Beasley	12115	July and Aug. 1970	60	2.5
Ft. Pickens	12120	July and Aug. 1970	61	2.0
Crystal Beach	12101	Sept. and Oct. 1969	60	2.5
" " "	"	Apr. and May 1970	61	2.5
MICHIGAN - LAKE MICHIGAN				
Porcupine	28410	May and June 1974	54	2.0
" " "	"	June and July 1974	51	2.0
Warren Dunes	28005	May and June 1974	51	2.0
" " "	"	June and July 1974	61	2.5
" " "	"	July and Aug. 1974	62	2.0
Muskegon	28030	June and July 1974	59	2.5
" " "	"	July and Aug. 1974	61	1.5
CALIFORNIA - PACIFIC COAST				
Manchester Beach	05023	*Aug. 1969	57	4.0
" " "	"	*Sept. 1969	50	2.5
" " "	"	*Aug. and Sept. 1969	107	2.5
" " "	"	*Sept. and Oct. 1969	82	2.5
PEG Pier, Pt. Mugu	05703	Jan. and Feb. 1975	56	2.5
PEG Pier, Pt. Mugu (Navy)	05702	June and July 1972	50	4.0
" " " " "	"	Aug. and Sept. 1972	54	4.4
" " " " "	"	Dec. 1972 and Jan. 1973	59	4.5
" " " " "	"	Jan. and Feb. 1973	55	2.5
" " " " "	"	Feb. and Mar. 1973	57	2.5
" " " " "	"	Mar. and Apr. 1973	59	2.5
" " " " "	"	Apr. and May 1973	55	2.0
" " " " "	"	May and June 1973	54	2.5
" " " " "	"	June and July 1973	53	3.0
" " " " "	"	July and Aug. 1973	53	3.5
" " " " "	"	Aug. and Sept. 1973	56	3.0
" " " " "	"	Sept. and Oct. 1973	60	2.0
" " " " "	"	Oct. and Nov. 1973	57	1.5
" " " " "	"	Nov. and Dec. 1973	56	2.0
" " " " "	"	Mar. and Apr. 1974	55	2.5
OREGON - PACIFIC COAST				
Bastendorf	43007	Feb. and Mar. 1979	59	1.5
" " "	"	Mar. and Apr. 1979	61	4.0
" " "	"	Apr. and May 1979	61	5.0
" " "	"	May and June 1979	61	5.5
" " "	"	Sept. and Oct. 1979	61	7.0
WASHINGTON - PACIFIC COAST				
Peacock Spit	57009	Jan. and Feb. 1979	60	3.0
" " "	"	Feb. and Mar. 1979	60	2.5
" " "	"	Mar. and Apr. 1979	61	5.2
" " "	"	Apr. and May 1979	60	5.2

* Twice-daily observations; all others once-daily.

authors. Autocorrelations were computed for observations ranging from once-daily (i.e., approximately every 24 hours) to twice-daily (i.e., assumed to be every 12 hours for computational purposes) to longer time intervals, k , as the sample size allowed ($k < n/4$ where n is the number of days representing the autocorrelation observation period). A typical example is illustrated in Figure 16.

The autocorrelation analysis suggests that the required interval between observations is, on the average about 2.86 days. However, with a standard deviation of 1.19 days for the 48 samples of Table 3 a more reasonable time interval may be suggested to be once every 24 hours or once every other day (i.e., $2.86 - 1.19 = 1.67 = 2$ days). This result means that while observations made more frequently than every other day may increase the probability that extreme values may be included in the record, the accuracy of the point estimators representing the normally expected wave climate at a site will probably not be greatly improved. Hence, the conclusion may be stated that for the average month represented by 30 days, approximately 15 observations are required in order to adequately sample the monthly shore-breaking wave activity provided that the individual observations are separated, on the average, by no more than 2 to 3 days.

Thompson and Harris (1972) conducted an autocorrelation analysis for nearshore wave gage data which measures the total spectra. Autocorrelations were computed for data separated by time intervals of from 4 to 140 hours. Thompson found that autocorrelations approached zero at about 1.5 days, which corroborates the autocorrelation function results for LEO data.

We are now in a position to want to know about the uncertainty associated with the mean of a time series, in this case a time series of LEO breaker heights. It is reasoned (Barry, 1978) that the uncertainty

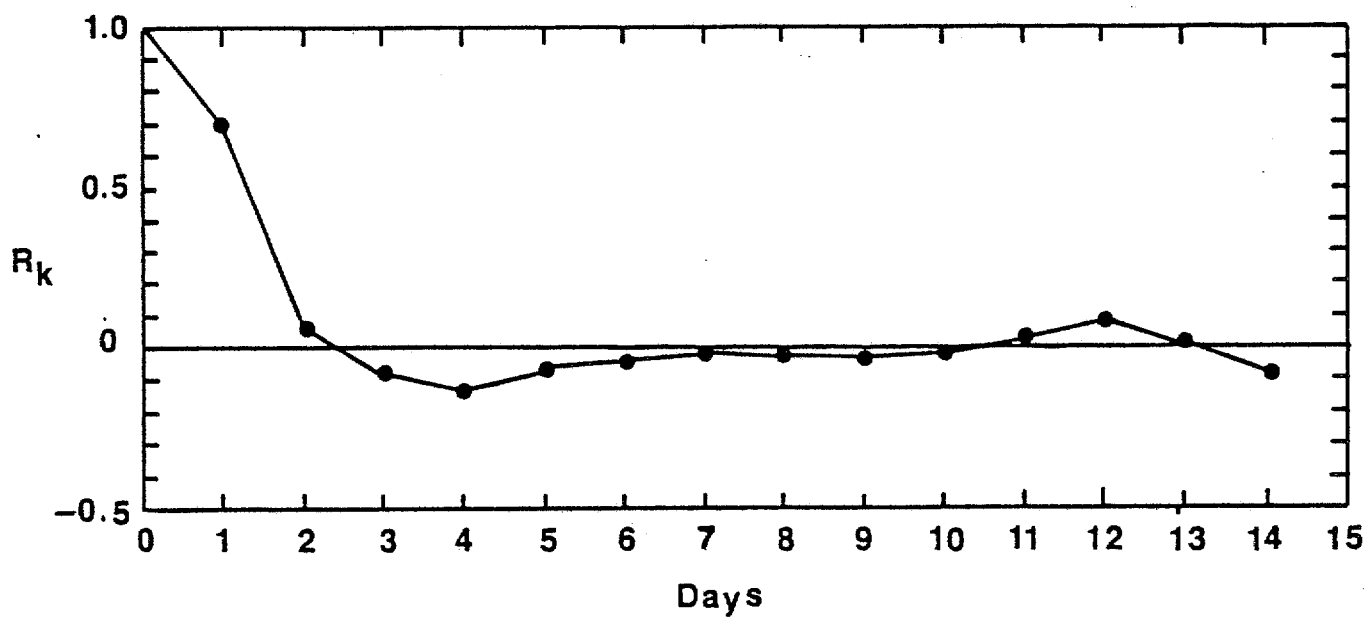


Figure 16. Autocorrelation analysis for shore-breaker heights at J. C. Beasley State Park, FL for July and August, 1970.

of the arithmetic mean of a series of measurements is much less than that of any single measurement. The standard error of the mean of a series, E_m , is given by:

$$E_m = \frac{\sqrt{\Sigma(E)^2}}{n} \quad (34)$$

where E is the probable observer error between the LEO and the actual breaker height. For the average observer error given by equation (32) which also represents one standard deviation about the mean for measured breaker data, the average error of the mean, E_{mavg} , may be given by:

$$E_{mavg} = \frac{\sqrt{\Sigma (0.21 H_{b \text{ LEO}})^2}}{n} \quad (35)$$

where $H_{b \text{ LEO}}$ is a single breaker height observation. Using the maximum error of the moment wave height, E_{max} , given by equation (33), the maximum error of the mean, E_{mmax} , may be given by:

$$E_{mmax} = \frac{\sqrt{\Sigma (0.62 H_{b \text{ LEO}})^2}}{n} \quad (36)$$

Free Shore-Incident Storm Waves

In practicable coastal engineering design solutions some upper measure of the wave height within the time series, not the average height, often needs to be considered. The height and type of the design wave should, ideally, be based on analytical procedure which includes determination of the accompanying storm surge, astronomical tides if storm impact should for some

not be considered a factor, wave setup, dune or bluff erosion (i.e., horizontal recession), and scour (i.e., vertical recession). Such involved analytical procedure, however, may at the outset require a less complicated check of what extremes in wave activity a particular locality is capable of supporting.

In addition, because design solutions are subject to economical constraints there may be a need, such as in regulatory responsibilities, to check for what wave height a particular structural solution has been designed. The results of a check may not necessarily involve additional expenditures, but allow for identification of alternative design solutions.

Assuming a Gaussian distribution, the maximum shore-breaker height of the distribution of a LEO time series record should be adequately represented by:

$$\bar{H}_{b\max \text{ LEO}} = \bar{H}_{b1 \text{ LEO}} = \bar{H}_{b\text{LEO}} + 3 s_t \quad (37)$$

The accuracy of equation (37) depends upon the number of elements (i.e., observations) made per monthly period; that is, whether large sampling statistics (i.e., $n \geq 30$) or small sampling statistics (i.e., $n \leq 30$) are under consideration. It has been established in a previous section that only 15 or greater observations are required per month to establish a representative average shore-breaker height. However, while a minimum of 15 observations may be adequate to specify the average value of the monthly record, the same consideration does not apply to equation (37) which may, ostensibly, require a more frequent observation schedule to reduce the amount of scatter. The relationship between $\bar{H}_{b\max \text{ LEO}}$ and $\bar{H}_{b \text{ LEO}} + 3 s_t$ for monthly data for several seasons from sites representing very different geomorphic conditions (i.e., Florida panhandle and California) is illustrated in Figure 17 (data listed in Table 4). The desirable goal

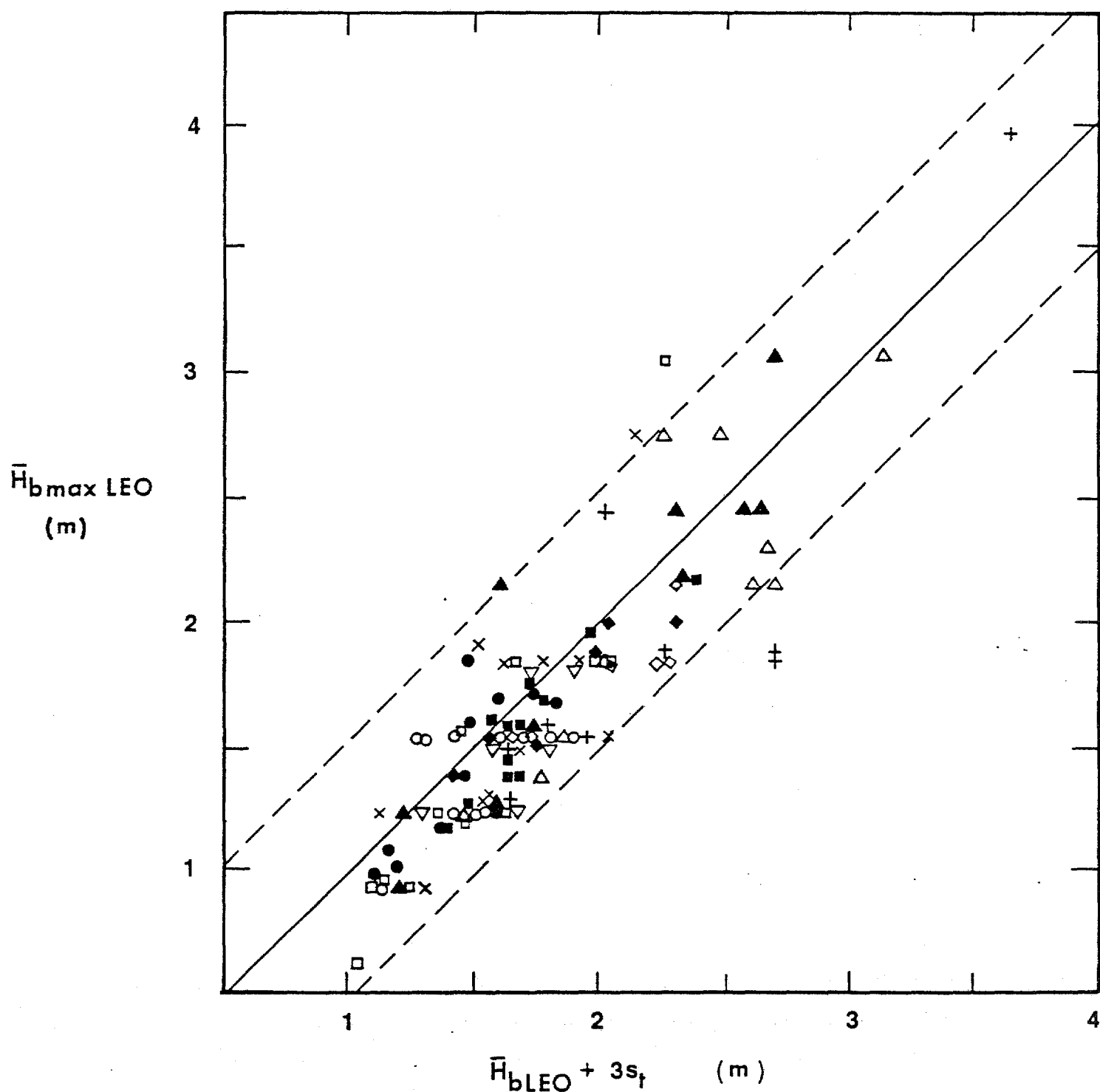


Figure 17. The maximum shore-breaker height of monthly LEO records, $\bar{H}_{b \max \text{ LEO}}$, versus the monthly average LEO height plus three standard deviations, $\bar{H}_{b \text{ LEO}} + 3s_t$. (Symbols identified in Table 4).

Table 4. Measured and predicted monthly LEO breaker height statistics.

Month/Year	n	\bar{H}_b LEO (m)	s_t (m)	s_{kt}	Kurt	\bar{H}_{bs} LEO (m)	\bar{H}_b LEO + 1.1 s_t (m)	\bar{H}_{bs} LEO from eq (40) (m)	\bar{H}_{b10} LEO (m)	\bar{H}_b LEO + 2 s_t (m)	\bar{H}_{b10} LEO from eq (40) (m)	\bar{H}_{bmax} LEO (m)	\bar{H}_b LEO + 3 s_t (m)	\bar{H}_{bmax} LEO from eq (40) (m)	Max %*
St. Andrews, Florida (12105) ○															
Sep. 1969	25	0.246	0.338	2.070	8.17	0.610	0.618	0.640	0.914	0.923	0.930	1.524	1.261	1.387	3.85
Oct. "	30	0.274	0.381	1.730	5.62	0.710	0.693	0.713	1.219	1.036	1.033	1.524	1.417	1.487	3.33
Nov. "	27	0.326	0.261	0.563	2.78	0.610	0.613	0.616	0.814	0.849	0.820	0.914	1.110	0.978	7.41
Dec. "	29	0.683	0.390	0.138	2.18	1.119	1.112	1.103	1.320	1.463	1.396	1.524	1.853	1.518	3.45
Jan. 1970	30	0.314	0.329	1.520	6.55	0.710	0.676	0.692	0.914	0.972	0.963	1.524	1.301	1.326	3.33
Feb. "	28	0.445	0.288	-0.024	2.09	0.744	0.762	0.753	0.914	1.020	0.972	0.914	1.308	1.039	14.29
Mar. "	31	0.668	0.323	0.583	2.74	1.036	1.023	1.024	1.219	1.314	1.265	1.524	1.637	1.448	3.23
Apr. "	28	0.576	0.262	0.207	2.96	0.847	0.864	0.860	1.015	1.100	1.049	1.219	1.362	1.131	3.57
May "	26	0.704	0.227	0.273	2.29	1.027	1.009	1.006	1.219	1.259	1.201	1.219	1.536	1.289	11.54
Jun. "	20	0.564	0.308	0.015	2.58	0.914	0.903	0.893	1.067	1.180	1.122	1.219	1.487	1.192	5.00
Jul. "	29	0.704	0.301	0.642	3.22	1.049	1.035	1.039	1.320	1.305	1.259	1.524	1.606	1.436	3.45
Aug. "	29	0.872	0.308	0.481	2.36	1.253	1.210	1.210	1.423	1.487	1.426	1.524	1.795	1.564	6.90
Grayton Beach, Florida (12110) □															
Sep. 1969	26	0.363	0.360	0.896	3.12	0.799	0.758	0.765	1.119	1.082	1.058	1.219	1.442	1.338	7.69
Oct. "	31	0.539	0.494	1.19	3.96	1.067	1.083	1.100	1.600	1.527	1.500	1.829	2.021	1.963	6.45
Nov. "	30	0.436	0.218	-0.311	2.61	0.643	0.676	0.664	0.710	0.872	0.823	0.914	1.091	0.823	3.33
Dec. "	30	0.732	0.515	3.29	14.60	1.186	1.298	1.378	1.929	1.762	1.811	3.048	2.277	2.914	3.33
Jan. 1970	31	0.411	0.239	0.886	3.16	0.701	0.675	0.680	0.914	0.890	0.866	0.914	1.129	1.049	12.90
Feb. "	28	0.588	0.335	0.464	2.68	0.948	0.957	0.957	1.219	1.259	1.210	1.219	1.594	1.381	14.29
Mar. "	30	0.692	0.222	0.584	3.32	0.981	0.936	0.939	1.119	1.135	1.088	1.219	1.357	1.201	6.67
Apr. "	30	0.610	0.272	1.12	5.00	0.914	0.909	0.924	1.119	1.155	1.125	1.524	1.427	1.325	3.33
May "	31	0.472	0.187	-1.02	3.00	0.610	0.678	0.655	0.610	0.847	0.783	0.610	1.034	0.674	61.29
Jun. "	28	0.418	0.289	0.151	2.11	0.743	0.735	0.728	0.914	0.995	0.954	0.914	1.284	1.055	14.29
Jul. "	30	0.488	0.390	2.59	9.40	0.881	0.917	0.960	1.423	1.268	1.283	1.829	1.658	1.951	6.67
Aug. "	30	0.619	0.454	1.02	4.05	1.152	1.118	1.131	1.625	1.527	1.490	1.829	1.981	1.878	6.67
Crystal Beach, Florida (12101) ×															
Sep. 1969	30	0.234	0.301	1.510	5.09	0.576	0.565	0.579	0.914	0.837	0.829	1.219	1.138	1.158	3.33
Oct. "	30	0.497	0.475	0.991	3.53	1.049	1.020	1.030	1.524	1.448	1.417	1.829	1.923	1.814	3.33
Nov. "	27	0.317	0.317	0.526	2.01	0.710	0.666	0.668	0.914	0.951	0.920	1.262	1.268	1.109	14.81
Dec. "	28	0.652	0.466	0.059	1.69	1.186	1.165	1.155	1.320	1.585	1.515	1.524	2.051	1.655	3.57
Jan. 1970	31	0.472	0.354	0.193	1.94	0.884	0.861	0.856	0.991	1.180	1.131	1.219	1.533	1.268	3.23
Feb. "	28	0.546	0.536	0.253	10.70	1.049	1.135	1.186	1.728	1.618	1.640	2.743	2.155	2.515	3.57
Mar. "	31	0.728	0.276	-0.578	3.04	0.975	1.032	1.009	1.067	1.280	1.198	1.219	1.555	1.113	6.45
Apr. "	30	0.661	0.344	-0.052	3.17	1.015	1.040	1.027	1.219	1.350	1.283	1.524	1.695	1.341	3.33
May "	36	0.619	0.396	0.553	3.79	1.082	1.055	1.055	1.372	1.411	1.362	1.829	1.807	1.588	2.78
Jun. "	30	0.527	0.457	0.871	2.84	1.119	1.030	1.039	1.524	1.442	1.405	1.524	1.849	1.756	10.00
Jul. "	31	0.433	0.399	1.670	6.06	0.884	0.872	0.893	1.295	1.231	1.222	1.829	1.631	1.698	3.23
J. C. Beasley, Florida (12115) +															
Oct. 1969	29	0.631	0.430	0.318	2.50	1.152	1.104	1.100	1.423	1.490	1.433	1.524	1.920	1.622	6.90
Nov. "	22	0.430	0.387	0.540	2.32	0.872	0.856	0.856	1.119	1.204	1.164	1.219	1.591	1.396	9.09
Dec. "	27	0.869	0.637	-0.048	1.64	1.591	1.569	1.551	1.829	2.143	2.042	1.829	2.780	2.198	11.01
Jan. 1970	25	0.671	0.530	0.235	1.91	1.295	1.254	1.247	1.423	1.731	1.661	1.829	2.262	1.884	4.00
Feb. "	21	0.899	0.933	1.92	6.45	1.871	1.925	1.984	2.844	2.765	2.765	3.962	3.697	3.993	4.76
Mar. "	20	1.052	0.558	-0.092	1.54	1.676	1.665	1.643	1.829	2.167	2.057	1.829	2.725	2.140	15.00
May "	25	0.573	0.369	0.366	3.23	0.951	0.979	0.975	1.219	1.311	1.259	1.524	1.679	1.430	4.00
Jun. "	29	0.314	0.475	1.56	4.69	0.914	0.837	0.856	1.423	1.265	1.259	1.829	1.740	1.783	3.45
Jul. "	30	0.314	0.576	2.68	9.59	0.881	0.948	0.994	1.829	1.466	1.497	2.438	2.042	2.426	3.33
Aug. "	31	0.433	0.457	0.76	2.38	1.006	0.936	0.942	1.295	1.347	1.314	1.524	1.804	1.640	3.23
Navarre Beach, Florida (12118) ▲															
Nov. 1969	27	0.475	0.384	2.780	13.30	0.780	0.898	0.942	1.119	1.244	1.265	2.134	1.628	1.960	3.70
Dec. "	25	0.512	0.363	0.921	2.74	0.951	0.911	0.920	1.219	1.237	1.207	1.219	1.600	1.494	16.00
Jan. 1970	27	0.326	0.298	0.800	2.71	0.643	0.654	0.658	0.914	0.923	0.899	0.914	1.221	1.116	14.81
Feb. "	20	0.351	0.294	1.040	4.49	0.710	0.673	0.683	0.194	0.938	0.917	1.219	1.231	1.170	5.00
Mar. "	27	0.744	0.335	0.392	2.36	1.119	1.113	1.109	1.320	1.414	1.356	1.524	1.750	1.500	3.70
Apr. "	29	0.936	0.466	1.530	4.65	1.423	1.449	1.460	1.829	1.868	1.811	2.438	2.335	2.143	3.45
May "	30	1.088	0.527	-0.015	3.75	1.591	1.668	1.649	2.033	2.143	2.036	2.438	2.670	2.128	3.33
Jun. "	29	0.950	0.579	0.539	3.42	1.490	1.487	1.487	2.033	2.009	1.939	2.438	2.583	2.271	3.45
Jul. "	23	0.711	0.511	1.500	6.10	1.397	1.472	1.503	2.234	2.070	2.048	3.043	2.774	2.780	3.57
Aug. "	31	0.600	0.570	0.605	2.71	1.250	1.227	1.231	1.600	1.740	1.689	2.134	2.310	2.048	3.23

*Max %: percentage of maximum heights in the monthly record.

Table 4. (cont.)

Month/Year	n	\bar{H}_b LEO (m)	s_t (m)	s_{kt}	Kurt	\bar{H}_{bs} LEO (m)	\bar{H}_b LEO + 1.1 s_t (m)	\bar{H}_{bs} LEO from eq (40) (m)	\bar{H}_{b10} LEO (m)	\bar{H}_b LEO + 2 s_t (m)	\bar{H}_{b10} LEO from eq (40) (m)	\bar{H}_{bmax} LEO (m)	\bar{H}_b LEO + 3 s_t (m)	\bar{H}_{bmax} LEO from eq (40) (m)	Max %*
Ft. Pickens, Florida (12120) ▽															
Sep. 1969	25	0.451	0.287	0.63	3.36	0.762	0.767	0.768	1.015	1.026	0.991	1.219	1.313	1.170	4.00
Mar. 1970	29	0.769	0.390	0.957	3.45	1.219	1.197	1.210	1.625	1.548	1.506	1.839	1.939	1.820	3.45
Apr. "	23	0.677	0.323	-0.223	2.09	1.003	1.032	1.015	1.119	1.323	1.250	1.219	1.646	1.262	8.70
May "	27	0.701	0.329	0.093	1.66	1.049	1.063	1.055	1.219	1.359	1.295	1.219	1.689	1.372	14.81
Jun. "	29	0.631	0.323	0.847	3.05	1.049	0.993	1.000	1.320	1.289	1.250	1.524	1.618	1.494	3.45
Jul. "	31	0.649	0.369	1.39	4.89	1.067	1.055	1.076	1.372	1.387	1.362	1.829	1.756	1.759	3.23
Aug. "	30	0.701	0.354	0.683	2.78	1.119	1.090	1.094	1.423	1.408	1.359	1.524	1.762	1.585	6.67
PEG Pier, California (05703) △															
Mar. 1972	18	0.981	0.704	1.700	5.35	1.676	1.756	1.801	2.743	2.390	2.371	3.048	3.094	3.231	5.56
Apr. "	20	0.951	0.263	0.018	1.62	1.271	1.241	1.228	1.372	1.478	1.399	1.372	1.741	1.399	10.00
May "	22	1.225	0.475	0.791	2.48	1.850	1.748	1.762	2.082	2.176	2.103	2.286	2.652	2.499	4.55
Jun. "	30	1.024	0.320	0.525	2.85	1.405	1.376	1.378	1.676	1.664	1.594	1.829	1.984	1.740	6.67
Jul. "	31	1.049	0.270	0.091	1.76	1.356	1.346	1.335	1.448	1.589	1.506	1.524	1.860	1.515	3.23
Aug. "	48	1.378	0.415	0.290	1.91	1.899	1.834	1.826	2.073	2.207	2.103	2.134	2.621	2.210	2.08
Sep. "	30	0.966	0.436	2.230	9.72	1.439	1.446	1.503	1.929	1.838	1.838	2.743	2.224	2.560	3.33
Oct. "	20	1.097	0.527	0.520	2.26	1.753	1.677	1.679	2.134	2.152	2.070	2.134	2.679	2.344	10.00
Nov. "	18	0.957	0.500	2.480	9.25	1.423	1.507	1.573	2.134	1.957	1.969	2.743	2.457	2.856	5.56
Dec. "	16	0.753	0.232	0.533	2.20	1.036	1.008	1.009	1.143	1.216	1.164	1.219	1.448	1.271	6.25
PEG Pier, California (05703) ●															
Jan. 1975	28	0.774	0.271	1.350	5.24	1.076	1.072	1.091	1.350	1.316	1.286	1.676	1.586	1.582	3.57
Feb. "	28	0.768	0.227	0.450	2.87	1.024	1.018	1.018	1.167	1.223	1.170	1.372	1.450	1.256	3.57
Apr. "	28	0.728	0.285	0.009	2.12	1.042	1.042	1.030	1.210	1.299	1.231	1.219	1.584	1.268	3.57
May "	32	0.753	0.239	2.740	13.10	0.991	1.016	1.067	1.164	1.231	1.241	1.829	1.470	1.768	3.13
Jun. "	21	0.744	0.140	0.722	2.75	0.905	0.897	0.902	0.997	1.023	0.981	1.067	1.163	1.055	4.76
Jul. "	27	0.713	0.255	2.010	7.31	0.985	0.994	1.027	1.271	1.223	1.213	1.646	1.478	1.618	3.70
Aug. "	22	0.747	0.122	0.156	2.50	0.896	0.881	0.375	0.945	0.990	0.936	0.975	1.112	0.917	9.09
Sep. "	23	0.869	0.314	1.100	3.48	1.241	1.214	1.231	1.524	1.497	1.454	1.676	1.811	1.740	4.35
Oct. "	19	0.741	0.153	-0.137	2.08	0.920	0.909	0.896	0.960	1.046	0.985	1.006	1.199	0.936	5.26
Nov. "	24	0.756	0.203	0.225	2.06	0.991	0.979	0.975	1.088	1.162	1.103	1.158	1.365	1.137	16.67
Dec. "	30	0.747	0.329	1.140	3.71	1.177	1.109	1.125	1.472	1.405	1.372	1.707	1.734	1.676	3.33
PEG Pier, California (05702) ◆															
Jun. 1972	23	0.832	0.203	0.603	3.62	1.036	1.055	1.058	1.198	1.237	1.186	1.372	1.440	1.280	4.35
Jul. "	26	0.887	0.228	0.711	3.27	1.161	1.138	1.143	1.320	1.344	1.292	1.524	1.572	1.423	3.85
Aug. "	27	0.966	0.335	0.834	2.83	1.353	1.335	1.344	1.625	1.637	1.582	1.829	1.972	1.820	3.70
Sep. "	27	1.000	0.250	0.984	3.29	1.286	1.275	1.289	1.524	1.500	1.451	1.676	1.750	1.655	3.70
Oct. "	20	0.823	0.302	0.934	3.48	1.195	1.156	1.167	1.524	1.428	1.384	1.524	1.730	1.622	12.00
Nov. "	25	1.158	0.384	-0.006	2.76	1.600	1.581	1.564	1.777	1.926	1.823	1.981	2.310	1.347	4.00
Dec. "	30	0.960	0.366	0.875	3.32	1.423	1.362	1.375	1.728	1.692	1.637	1.981	2.057	1.908	3.33
PEG Pier, California (05702) ■															
Jan. 1973	29	0.893	0.271	0.515	2.60	1.222	1.191	1.192	1.423	1.435	1.375	1.524	1.706	1.494	10.34
Feb. "	26	1.183	0.402	0.873	3.28	1.673	1.625	1.640	2.021	1.987	1.920	2.164	2.390	2.219	3.85
Mar. "	31	0.927	0.234	0.901	3.34	1.198	1.184	1.195	1.393	1.395	1.347	1.524	1.630	1.521	9.68
Apr. "	28	0.786	0.237	0.123	2.14	1.067	1.048	1.039	1.167	1.261	1.198	1.219	1.499	1.225	14.29
May "	27	0.829	0.287	0.391	2.11	1.167	1.145	1.143	1.320	1.403	1.341	1.372	1.690	1.451	3.70
Jun. "	27	0.933	0.347	1.010	3.79	1.341	1.315	1.329	1.615	1.628	1.579	1.951	1.975	1.871	3.70
Jul. "	26	0.835	0.226	0.462	5.29	1.027	1.084	1.085	1.219	1.287	1.231	1.524	1.514	1.314	3.35
Aug. "	25	0.802	0.311	1.510	4.93	1.146	1.144	1.170	1.494	1.423	1.399	1.737	1.734	1.771	4.00
Sep. "	29	0.811	0.278	-0.241	2.45	1.094	1.116	1.097	1.271	1.366	1.286	1.372	1.644	1.256	3.45
Oct. "	31	0.738	0.216	-0.173	2.56	0.978	0.976	0.963	1.088	1.170	1.103	1.158	1.387	1.076	3.23
Nov. "	26	0.838	0.267	0.192	2.54	1.143	1.132	1.125	1.289	1.372	1.305	1.433	1.639	1.359	3.85
Dec. "	30	0.866	0.314	0.933	3.09	1.268	1.211	1.222	1.524	1.494	1.448	1.676	1.807	1.695	3.33
Manchester State Beach, California (05023) ◇															
May 1968	35	1.045	0.415	-0.191	2.35	1.469	1.501	1.478	1.676	1.875	1.771	1.829	2.289	1.768	5.71
Jun. "	45	0.981	0.248	-0.179	3.19	1.262	1.254	1.237	1.341	1.477	1.390	1.524	1.725	1.335	4.44
Jul. "	56	1.012	0.216	-0.450	9.66	1.237	1.250	1.198	1.271	1.445	1.317	1.524	1.661	0.978	1.79
Aug. "	57	1.053	0.332	0.831	3.24	1.439	1.423	1.436	1.777	1.722	1.661	1.829	2.054	1.896	3.77
Sep. "	50	1.109	0.402	0.577	3.14	1.564	1.552	1.554	1.951	1.914	1.838	2.134	2.316	2.048	1.00
Oct. "	53	1.247	0.341	-1.13	5.21	1.576	1.622	1.564	1.875	1.929	1.777	1.829	2.271	1.442	5.17

* Max %: percentage of maximum heights in the monthly record.

is to reduce the amount of scatter in Figure 17 such that prediction of $\bar{H}_{bmax\ LEO}$ is more reliable. In the same manner, some other measures may be of value such as the following fitted relationships:

$$\bar{H}_{b10\ LEO} = \bar{H}_b\ LEO + 2 s_t \quad (38)$$

and

$$\bar{H}_{bs\ LEO} = \bar{H}_b\ LEO + 1.1 s_t \quad (39)$$

illustrated in Figures 18 and 19, respectively, where $\bar{H}_{b10\ LEO}$ is the average of the highest 10% of the recorded average shore-breaker heights, and $\bar{H}_{bs\ LEO}$ is the average of the highest one-third heights of the record.

It is quite obvious from the figures that the amount of scatter diminishes from $\bar{H}_{bmax\ LEO}$ to $\bar{H}_{bs\ LEO}$. Equations (37), (38) and (39) are now available to determine a continuum relationship.

In addition to knowledge that smaller breaker heights are common and large values relatively rare, one should note that because there are no negative values the distribution of a monthly record can be truncated at zero when calm conditions prevail. One must, therefore, understand that a skewed distribution is the rule rather than the exception. Using the data of Table 4, the following equation has been developed for prediction of the shore-breaker height of the monthly LEO record corresponding to the per cent occurrence:

$$\bar{H}_{b\alpha\ LEO} = \left(\bar{H}_b\ LEO + \Phi s_t \right) \left[\left(1.0 - 0.0075 \Phi^3 \right) + 0.0184 \Phi^{1.92} s_{kt} \right] \quad (40)$$

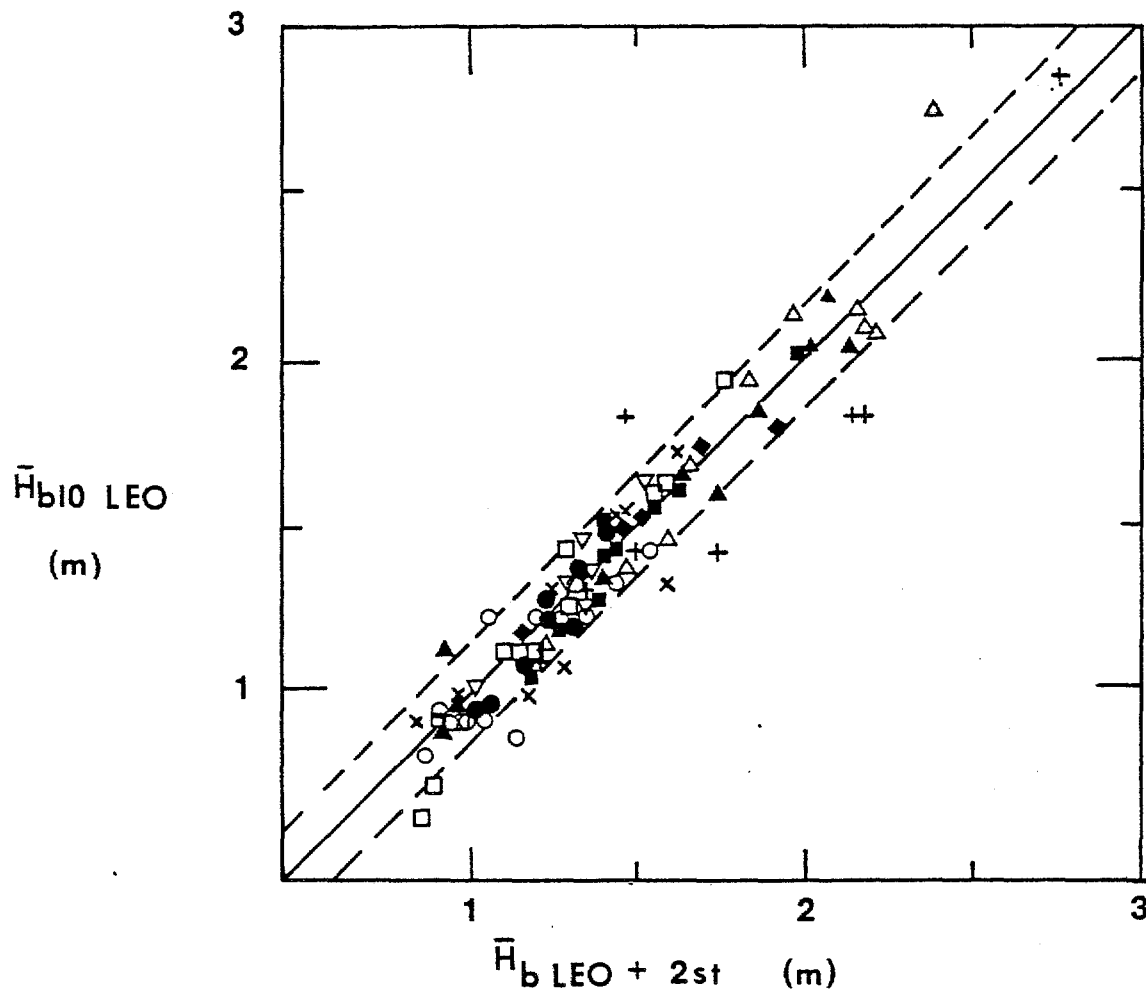


Figure 18. The average of the highest one-tenth shore-breaker heights of monthly LEO records, $\bar{H}_b \text{ LEO}$, versus $\bar{H}_{b10} \text{ LEO}$ predicted from equation (40). (Symbols identified in Table 4).

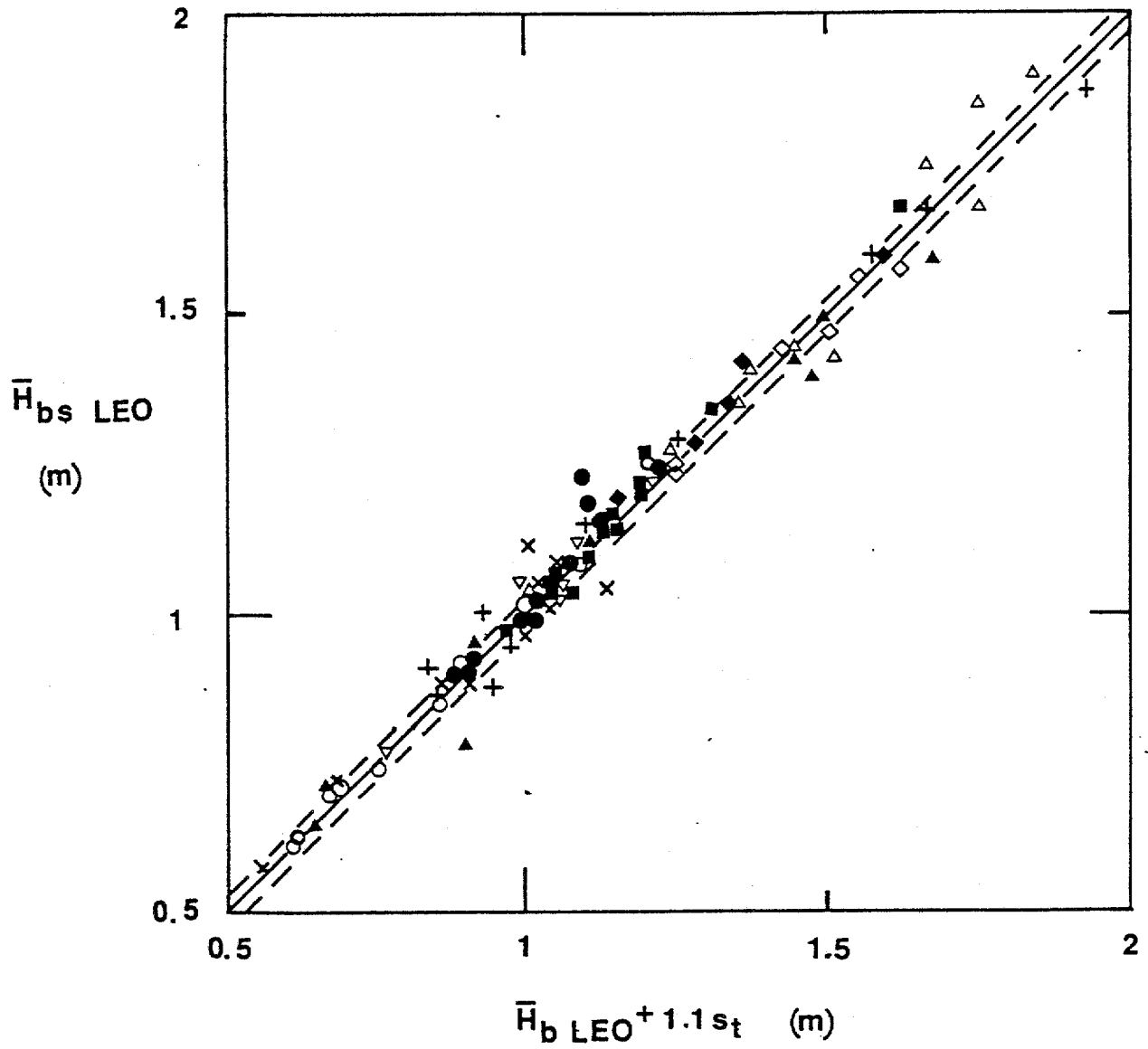


Figure 19. The average of the highest one-third of shore-breaker height of monthly LEO records, $\bar{H}_{bs \text{ LEO}}$, versus the monthly average LEO height plus 1.1 standard deviation, $\bar{H}_b \text{ LEO} + 1.1 s_t$. (Symbols identified in Table 4).

where

$$\Phi = 1.0 + \frac{5}{2} p^8 \quad \left\| \quad 0.5 \leq P \leq 1.0 \right. \quad (41)$$

and where s_{kt} is the skewness of the distribution, P is the percentage of the distribution considered, and $\alpha = 100(1 - P)$. For example, where $P = 0.80$ then $\alpha = 20$ and equation (40) predicts the average height of the highest 20% of the recorded breaker heights. Note that in addition to predicting the average of the time series for that upper portion of the distribution considered, the result in a moment estimator is an average and equations (8) through (13) are to be applied to determine higher design breaker heights.

Equation (40) is tested in Figures 20, 21 and 22. Comparison of Figures 17 and 20 for $\bar{H}_{bmax} LEO$ illustrates that by incorporating the skewness of the time series equation (40) significantly reduces the amount of scatter not accounted for by equation (37). In fact, the scatter in terms of the average absolute deviation plus three standard deviations indicates that equation (40) reduces the amount of scatter associated with equation (37) by 285%. Statistics leading to this result are given in Table 5, where the maximum scatter associated with equation (37) is ± 0.542 m (± 1.778 feet) while for equation (40) the maximum scatter is only ± 0.1903 m (± 0.6243 feet).

Comparison of Figures 18 and 21 for $\bar{H}_{b10} LEO$ does not give the impression that equation (40) results in less scatter than equation (38). However, statistics from Table 5 suggest that equation (40) reduces the amount of scatter by 133%, and the maximum scatter for equation (29) is ± 0.1556 m (± 0.5104 feet) while for equation (40) it is ± 0.117 m (± 0.384 feet).

Table 5. Selected statistics for evaluation of LEO breaker height time series distribution prediction.

	Observed \bar{H}_{bmax} LEO				Observed \bar{H}_{b10} LEO				Observed \bar{H}_{bs} LEO			
	MAD (m)	s_{MAD} (m)	Maximum Scatter (m)	r	MAD (m)	s_{MAD} (m)	Maximum Scatter (m)	r	MAD (m)	s_{MAD} (m)	Maximum Scatter (m)	r
\bar{H}_b LEO + 3 s_t (m)	0.2462 (0.8078)	0.0986 (0.3234)	0.5420 (1.7780)	0.8660	—	—	—	—	—	—	—	—
\bar{H}_{bmax} LEO from equation (40) (m)	0.1084 (0.3558)	0.0273 (0.0895)	0.1903 (0.6243)	0.9650	—	—	—	—	—	—	—	—
\bar{H}_b LEO + 2 s_t (m)	—	—	—	—	0.0942 (0.3091)	0.0205 (0.0671)	0.1556 (0.5104)	0.9539	—	—	—	—
\bar{H}_{b10} LEO from equation (40) (m)	—	—	—	—	0.0733 (0.2406)	0.0146 (0.0478)	0.1170 (0.3840)	0.9698	—	—	—	—
\bar{H}_b LEO + 1.1 s_t (m)	—	—	—	—	—	—	—	—	0.0316 (0.1036)	0.0022 (0.0073)	0.0382 (0.1254)	0.9905
\bar{H}_{bs} LEO from equation (40) (m)	—	—	—	—	—	—	—	—	0.0354 (0.1161)	0.0042 (0.0136)	0.0475 (0.1559)	0.9855

Notes:

1. MAD = mean absolute deviation.
2. s_{MAD} = sample standard deviation of the MAD.
3. Maximum Scatter = $\pm [MAD + 3(s_{MAD})]$, plotted in Figures 16 through 22 as dashed lines.
4. r = Pierson product-moment correlation coefficient.
5. Numbers in parentheses in feet.

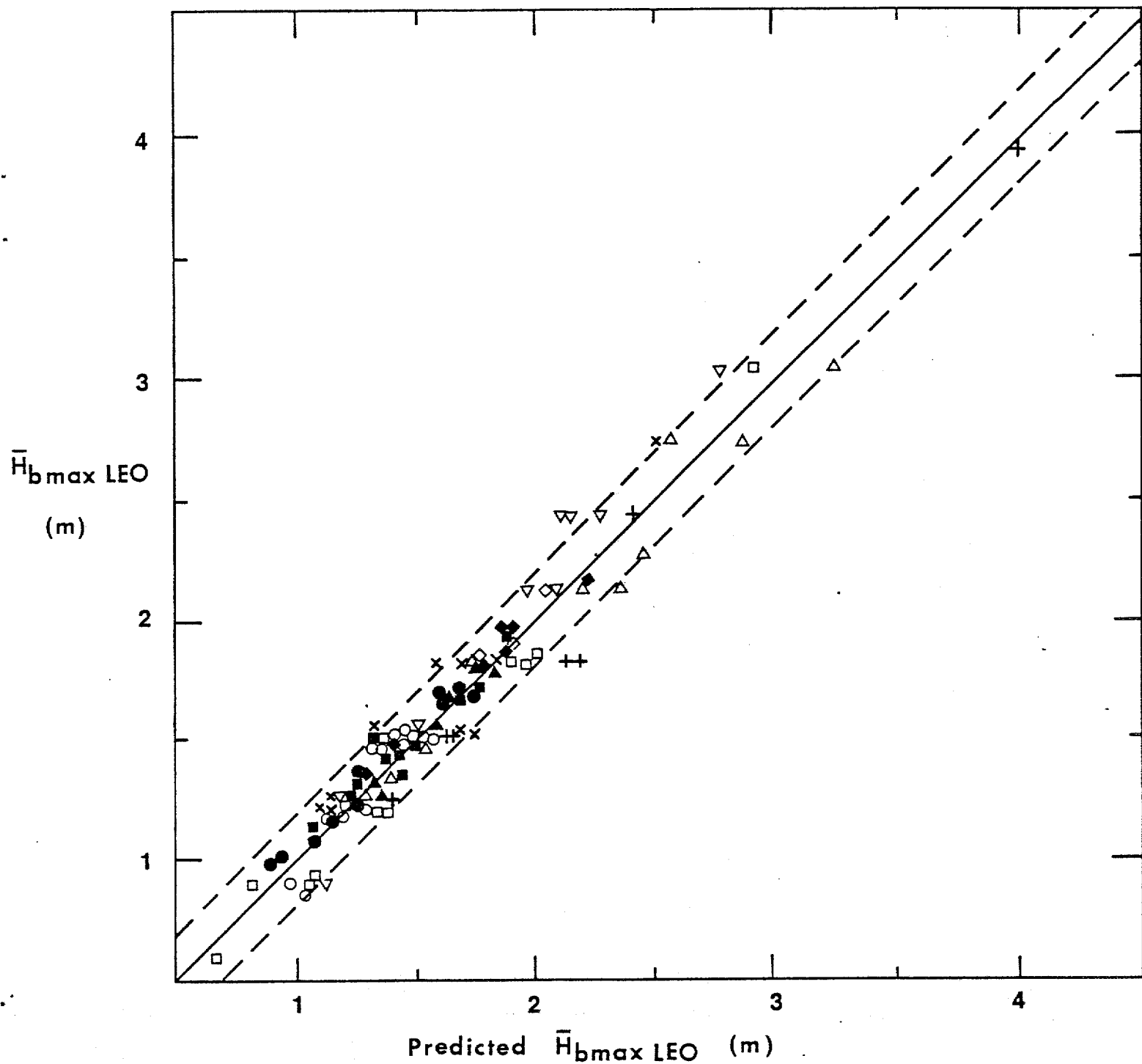


Figure 20. The maximum shore-breaker height of monthly LEO records, $\bar{H}_{bmax\ LEO}$, versus $\bar{H}_{bmax\ LEO}$ predicted from equation (40). (Symbols identified in Table 4).

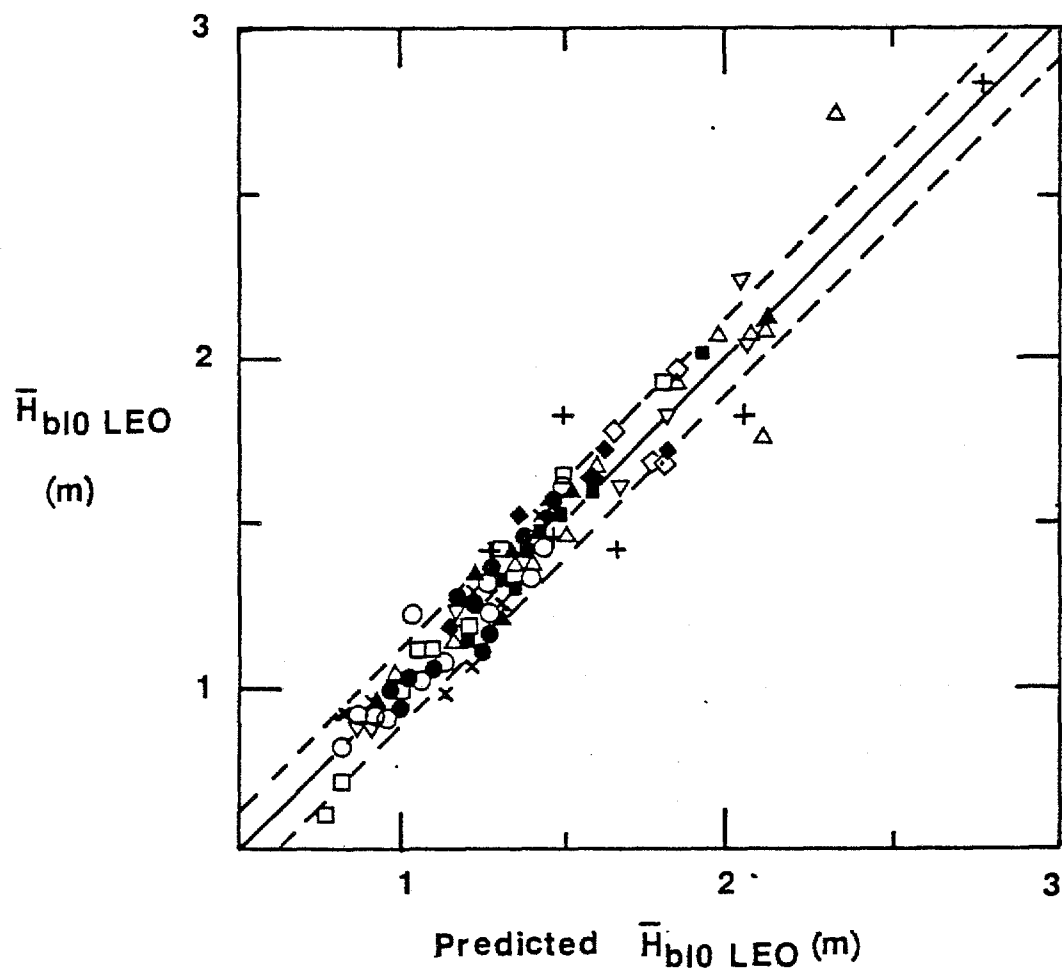


Figure 21. The average of the highest one-tenth shore-breaker heights of monthly LEO records, $\bar{H}_{b10 \text{ LEO}}$, versus the monthly average LEO height plus two standard deviations, $\bar{H}_b \text{ LEO} + 2 s_t$. (Symbols identified in Table 4).

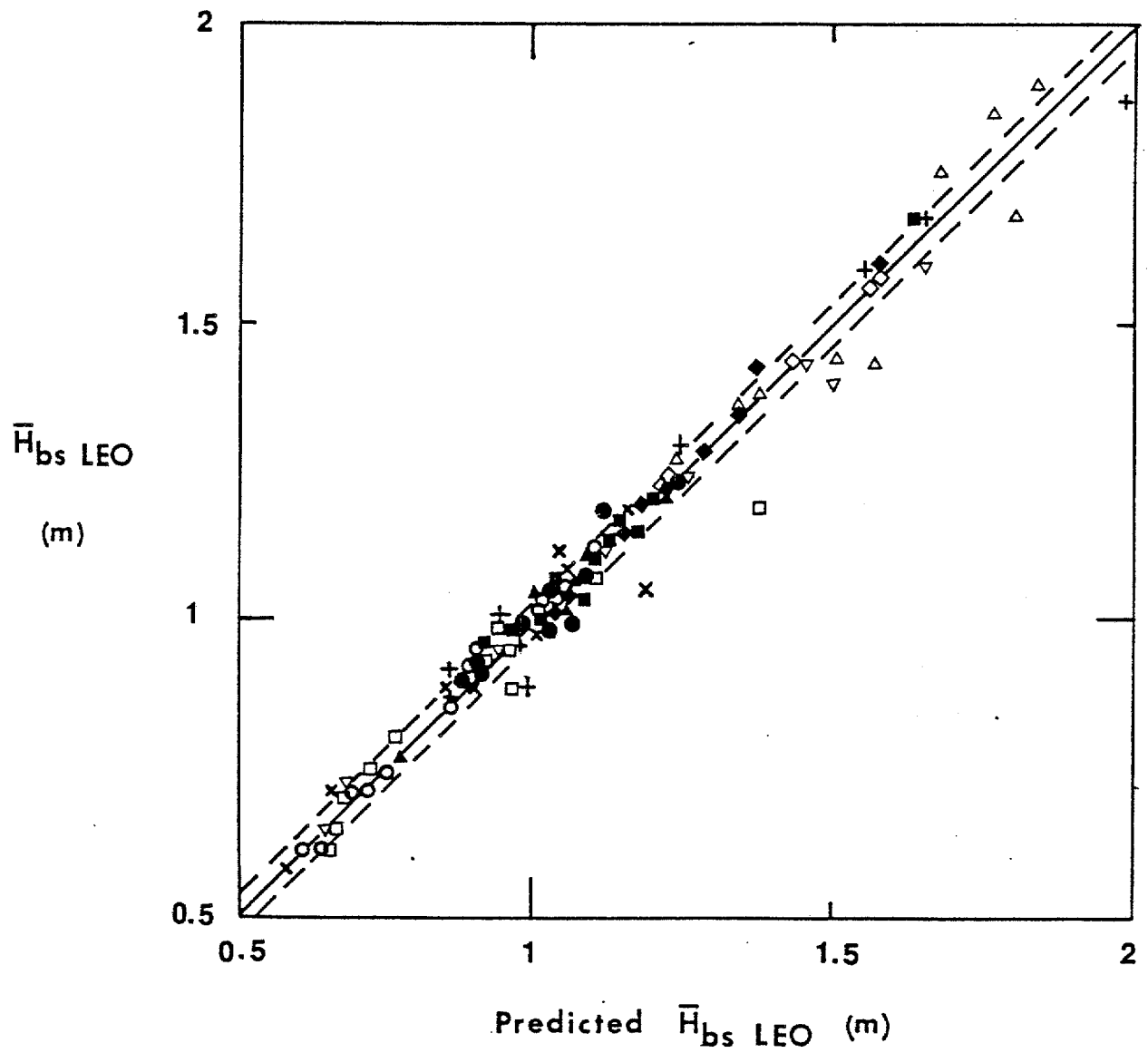


Figure 22. The average of the highest one-third shore-breaker heights of monthly LEO records, $\bar{H}_{bs} \text{ LEO}$, versus $\bar{H}_{bs} \text{ LEO}$ predicted from equation (40). (Symbols identified in Table 4).

Figures 19 and 22 for $\bar{H}_{bs \text{ LEO}}$, as for the previous case, do not appear to suggest that equation (40) reduces the amount of scatter associated with equation (39), which statistics from Table 5 confirm. However, the amount of scatter associated with both equations is minimal.

Of special importance is the apparent capability of equation (40) to successfully predict the maximum shore-breaking wave height, $\bar{H}_{bmax \text{ LEO}}$, of the monthly series, despite the fact that for the data of this study $\bar{H}_{bmax \text{ LEO}}$ comprised from 1.79 to 61.29% of the monthly record (Table 4). Due to the importance of \bar{H}_{bmax} in design applications, a simplified form of shore-incident storm wave may be given by:

$$\bar{H}_{bmax \text{ LEO}} = \left(\bar{H}_b \text{ LEO} + 3 s_t \right) \left(\frac{4}{5} + \frac{2 \pi}{41} s_k \right) \quad (42)$$

Description of a probability distribution requires four statistical measures: the mean, the standard deviation, skewness and kurtosis (determined using moment measures in this work). Mathematical treatments in this section have indicated a useful relationship between the first three measures (i.e., equations (40) and (42)). Hence, in addition, it may be of benefit to also look at the kurtosis. Figure 23 is a plot of the skewness (degree of curve asymmetry) versus the kurtosis (degree of curve peakedness) for, in this case, the Gaussian distribution. A trend is noted from which:

$$\text{Kurt} = 2.0 + 1.25 s_{kt}^2 \quad (43)$$

may be suggested. The usefulness of equation (43) is not at this time clear, but because of the trend is deemed important to report.

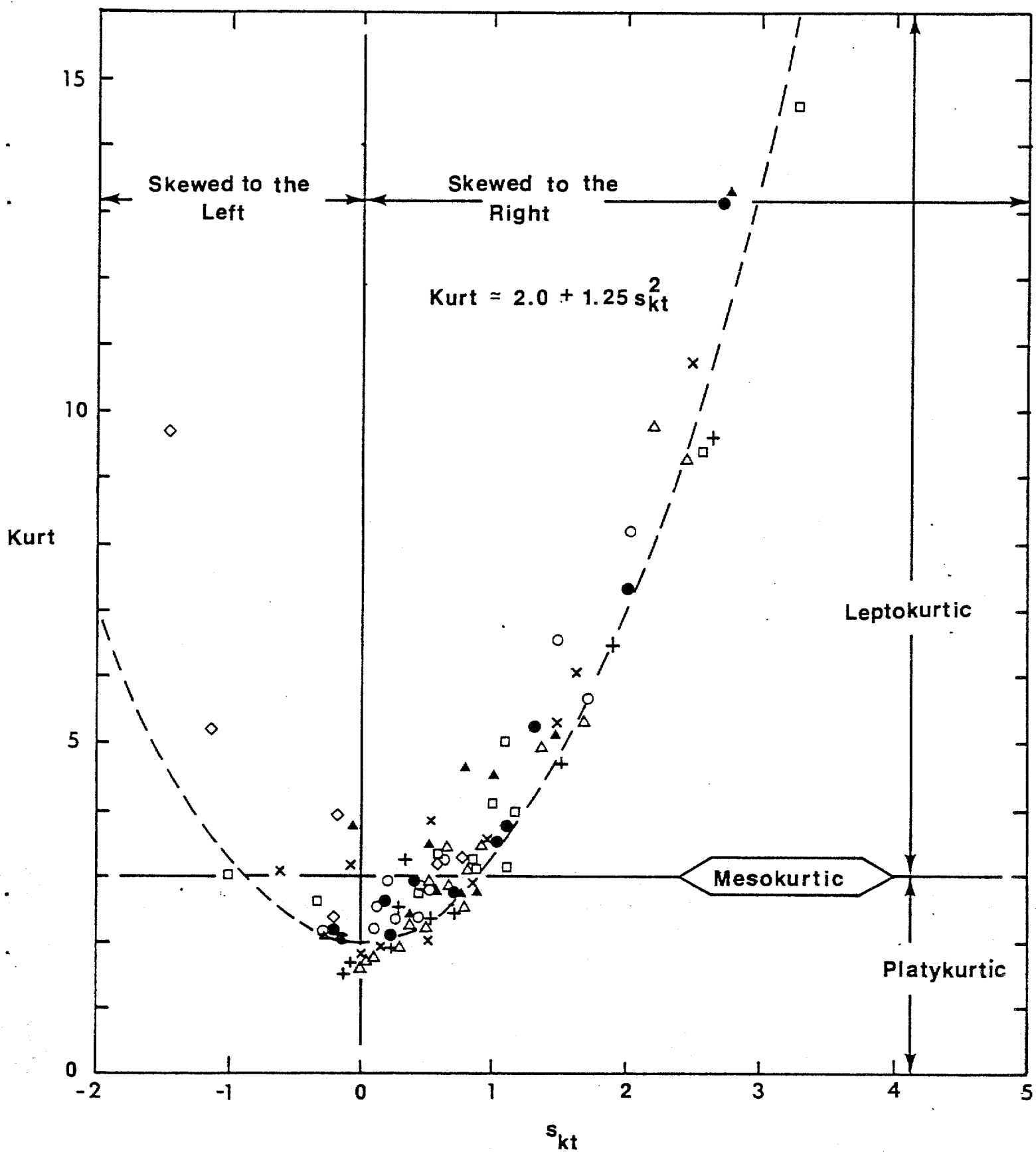


Figure 23. Skewness, s_{kt} , versus kurtosis, kurt, for monthly LEO height data (Symbols identified in Table 4).

Where daily shore-breaker height data is available to the coastal engineer, equations (40) and (42) are not needed. However, if monthly point estimators, only, are available, then they will have useful value. Therefore, the recommendation is made that monthly LEO summary reports also provide a listing of the skewness and, perhaps, the kurtosis.

CONCLUSIONS

Madsen (1976) states "..... the ultimate limitation of any wave theory based on potential theory is given by the conditions at which the wave breaks". In fact, at the present time there are no published theories for replicating the behavior of shore-breaking and shore-broken waves. Even so, certain persistent discrepancies appear in the literature.

As an example, suppose that a particular coastal engineering design solution depends on the knowledge of expected erosion of a protective foredune due to the impact of a selected return design storm or hurricane event. For such conditions, the immediate possibility occurs that multiple longshore bars are formed to cause multiple shore-breaking episodes as discussed by Balsillie (1980, in manuscript) and Balsillie and Carter (1980). Let us assume that for local subaqueous topographic conditions encountered and the determined incident design wave characteristics, three longshore bars are formed. Now, three shore-breaking episodes will occur (numbered consecutively from offshore to onshore) with a fourth, and final shore-breaking episode occurring at the shoreline. It is this fourth, final shore-breaking and the runup which it generates that will erode the dune. Even though we have already conceded that existing theories are no longer valid shoreward of the first shore-breaking episode, it is surprising that various investigators persist to record in the literature prediction methodology for various littoral processes, such as runup mechanics, which

are based on consideration of classical wave theories (see Balsillie and Carter (1980) for discussion). The use of such theories to solve littoral zone problems, where no other option is available can be understood, but only if one is sure that every effort has been made to ensure that attendant littoral processes do not unduly compound uncertainties already inherent in the selected theory.

In order to be in a position to replicate highly complex littoral zone mechanics, more knowledge, and perhaps even more importantly, identification of the managable components in littoral behavior (see Balsillie and Carter, 1980, p. 281-305) to facilitate mathematical quantifications, are required. This paper has been written to not only identify the viability of observed shore-breaker height data, but in doing so has revealed an additional number of results which may be of value in advancing understanding of the littoral environment. Conclusions are:

1. The original work by Munk (1949) upon which the definition of significant wave height is based, at least for shore-breaking waves is incorrect. Munk reports that when the breaker height is visually estimated by an experienced observer, the result corresponds to the average of the highest 30% (and not one-third) of the actual wave record. Using regression techniques, however, the authors found that experienced observers report the average breaker height.
2. While the Rayleigh distribution may provide an "..... excellent approximation....." (Harris, 1972) for a moment wave height record representing deeper water waves (i.e., where water depths are sufficient to support several to many wave trains), the shore-breaking moment distribution is successfully

represented by the Gaussian distribution (Figure 14). The difference presumably occurs because shore-breaking waves are depth limited for individual wave trains.

3. Deeper water spectral records (e.g., most gage records) which represent multiple wave trains and shore-breaking records which represent single wave trains, do not have the same relating moment statistics for determination of extreme values. Deeper water spectral record relating moment statistics are given by equations (1) through (7). Significantly different relating moment statistics apply to shore-breaking moment records, given by equations (8) through (13). A continuum relationship for each is closely approximated by equations (15) and (16). When applying such relating statistics in design problems one must be careful to choose the proper wave environment, as discussed in text using the longshore transport example.
4. The error associated with a single visual shore-breaker height is suggested to be given by equations (32) and (33). The average error given by equation (32) is no worse than the expected error associated with classical wave theories (i.e., about $\pm 20\%$). The maximum error from equation (33) is at first glance significantly larger; however, since we are mainly interested in results from a time series, the mean value of the series will be much less than the error of a single report. Time series errors may be computed using equations (35) and (36).
5. The number of observations required in a LEO effort to produce reliable point estimators for breaker height has remained unsubstantiated. An autocorrelation was conducted for a significant amount of LEO data from a wide range of localities

(Table 3). It was found that a minimum of 15 observations are required per month to obtain reliable point estimators, provided that they are evenly distributed across the time series record.

6. It is determined that monthly time series records from a LEO type program successfully represent normally expected wave activity and free shore-incident storm waves, but not forced shore-incident storm waves. Even so, in design problems some extreme wave height value is usually sought. Equation (40) has been developed which appears to provide reasonable values of $\bar{H}_{b\alpha}$ LEO for the monthly time series record where $\alpha = (1 - P)$ for a probability domain of $0.5 \leq 1.0$, and is useful where only monthly point estimators are available. The recommendation is made that in addition to monthly means and standard deviations currently provided in LEO summary reports, the third moment (skewness) and possibly, the fourth moment (kurtosis) are also listed. Further investigation concerning the usefulness of kurtosis and other considerations of time-series analytical methods for LEO data are warranted.

ACKNOWLEDGEMENTS

Special acknowledgement is given to Dr. C. Carter who loyally participated with the authors in obtaining the field data used in this study. Acknowledgement of other participants has been given in previous publications by the authors. Special acknowledgement is also given to J. J. Wenger who provided invaluable assistance in identifying psychological research relating to human visual perception of objects and for review of the pertinent text.

With few exceptions, figures were drafted by L. J. Penquite. Typing of the final manuscript was accomplished by L. G. Perritte.

REFERENCES

- Antis, S. M., Shöpland, G. D., and Gregory, R. L., 1961, Measuring visual constancy for stationary or moving objects: Nature, v. 191, p. 416-417.
- Balsillie, J. H., in manuscript, Wave length and wave celerity during shore-breaking.
- Balsillie, J. H., in manuscript, The transformation of the wave height during shore-breaking: the alpha wave peaking process.
- Balsillie, J. H., in manuscript, Wave crest elevation above the design water level during shore-breaking.
- Balsillie, J. H., 1980, The peaking of waves accompanying shore-breaking: Proceedings of a Symposium on Shorelines Past and Present, Department of Geology, Florida State University, Tallahassee, p. 183-247.
- Balsillie, J. H., 1977a, Prediction of longshore transport in the littoral zone with and without the use of breaking wave angles: Coastal Sedimentology, Department of Geology, Florida State University, Tallahassee, FL, p. 81-130.
- Balsillie, J. H., 1977b, Accuracy of a computer refraction simulation for predicting breaking wave characteristics and littoral transport: Coastal Sedimentology, Department of Geology, Florida State University, Tallahassee, FL, p. 131-172.
- Balsillie, J. H., 1975a, Analysis and interpretation of littoral environment observation (LEO) and profile data along the western panhandle coast of Florida: Coastal Engineering Research Center, Technical Memorandum No. 49, 104 p.
- Balsillie, J. H., 1975b, Surf observations and longshore current prediction: Coastal Engineering Research Center, Technical Memorandum No. 58, 39 p.
- Balsillie, J. H., et al., 1976, Wave parameter gradients along the wave ray: Marine Geology, v. 22.
- Balsillie, J. H., and Carter, R. W. G., 1980, On the run-up resulting from shore-breaking wave activity: Proceedings of a Symposium on Shorelines Past and Present, Department of Geology, Florida State University, Tallahassee, p. 269-342.
- Barry, B. A., 1978, Errors in Practical Measurement in Science, Engineering and Technology, John Wiley and Sons, Inc., New York.
- Berg, D. W., 1968, Systematic collection of beach data: Proceedings of the 11th Conference on Coastal Engineering, Chap. 17, p. 273-297.
- Bruno, R. O., 1971, Longshore current system, Panama City to Pensacola: M. S. Thesis, Department of Geology, Florida State University, Tallahassee, FL.

- Bruno, R. O., and Hiipakka, L. W., 1973, Littoral Environment Observation Program in the State of Michigan: Proceedings, 16th Conference on Great Lakes Research, International Association on Great Lakes Research, p. 492-507.
- Descartes, 1637, Dioptrics.
- DeWall, A. E., and Richter, J. J., 1977, Beach and Nearshore processes in southeastern Florida: Coastal Sediment '77, American Society of Civil Engineers Specialty Conference, p. 425-443.
- Goodnight, R. C., and Russell, T. L., 1963, Investigation of the statistics of wave heights: Journal of the Waterways and Harbors Division, No. WW2 p. 29-54.
- Grant, U. S., 1943, Waves as a transporting agent: American Journal of Science, v. 241, p. 117-123.
- Gregory, R. L., 1978, Eye and Brain, McGraw-Hill, Inc., New York, 256p.
- Gregory, R. L., and Ross, H. E., 1964a, Visual constancy during movement: Perceptual and Motor Skills, v. 18, p. 3-8.
- Gregory, R. L., and Ross H. E., 1964b, Visual constancy during movement: Perceptual and Motor Skills, v. 18, p. 23-26.
- Harris, D. L., 1972, Characteristics of wave records in the coastal zone: [In] Waves on Beaches and Resulting Sediment Transport, Academic Press, New York, p. 1-51.
- Inman, D. L., and Bagnold, D. L., 1963, Littoral processes: [In] The Sea, Interscience, New York, v. 1, p. 529-549.
- Kinsman, B., 1965, Wind Waves, Prentice-hall, Inc., Englewood Cliffs, new Jersey.
- Komar, P. D., 1976, Beach Processes and Sedimentation, Prentice-Hall, Inc. Englewood Cliffs, New Jersey.
- Komar, P. D., 1971, The mechanics of sand transport on beaches: Journal of Geophysical Research, v. 76, no. 3, p. 713-721.
- Komar, P. D., 1969, The longshore transport of sand on beaches: Ph.D. dissertation, University of California, San Diego, CA., 143p.
- Krumbein, W. C., and Graybill, F. A., 1965, An Introduction to Statistical Models in Geology, McGraw-Hill, Inc., New York, 475p.
- Lonquet-Higgins, M. S., 1972, Recent progress in the study of longshore currents: [In] Waves on Beaches and Resulting Sediment Transport, Academic Press, Inc., New York, p. 203-248.
- Lonquet-Higgins, M. S., 1970, Longshore currents generated by obliquely incident sea waves, parts 1 and 2: Journal of Geophysical Research, v. 75, no. 33, p. 6778-6801.

- Madsen, O. S., 1976, Wave climate of the continental margin: elements of its mathematical description: [In] Marine Sediment Transport and Environmental Management, John Wiley and Sons, New York, Chapter 6, p. 65-90.
- McClenan, C. M., and Harris, D. L., 1975, The use of aerial photography in the study of wave characteristics in the coastal zone: U. S. Army Coastal Engineering Research Center, Tech. Memo. No 48.
- McCowan, J., 1894, On the highest wave of permanent type: Philosophical Magazine Edinburgh, v. 32, p. 351-358.
- Mooers, C. N. K., 1976, Wind-driven currents on the continental margin: [In] Marine Sediment Transport and Environmental Management, John Wiley and Sons, New York, p. 29-52
- Munk, W. H., 1944, Proposed uniform procedure for observing waves and interpreting instrument records: [declassified U.S. Govt. document], Scripps Institution of Oceanography, S.I.O. Report No. 26.
- Ricker, W. E., 1973, Linear regressions in fishery research: Journal of the Fisheries Research Board of Canada, v. 30, no. 3, p. 409-434.
- Robinson, D. A., and Jones, C. M., 1977, Queensland volunteer Coastal Observation Programme -- Engineering: Proceedings of the 3rd Australian Conference on Coastal and Ocean Engineering, p. 88-95.
- Schneider, C., 1977, Visual surf observations/Marineland experiment: Coastal Sediment '77, American Society of Civil Engineers Specialty Conference, p. 1086-1100.
- Schneider, C., and Weggel, J. R., 1980, Visually observed wave data at Pt. Mugu, Calif.: Proceedings of the 17th International Coastal Engineering Conference, chap. 23, p. 381-393.
- Szuwalski, A., 1970, Littoral Environment Observation Program in California, preliminary report: U.S. Army, Coastal Engineering Research Center, Misc. Paper 2-70.
- Tanner, W. F., 1960, Florida coastal classification: Transactions of the Gulf Coast Association of Geologic Societies, v. 10, p. 259-266.
- Thompson, E. F., 1977, Wave climate at selected locations along U.S. coasts: U.S. Army, Coastal Engineering Research Center, Tech. Report No. 77-1, 364p.
- Thompson, E. F., and Harris, D. L., 1972, A wave climatology for U.S. coastal waters: Offshore Technology Conference, Paper No. OTC1693.
- Thouless, R. H., 1932, Individual differences in phenomenal regression: British Journal of Psychology, v. 22, p. 216-241.

Thouless, R. H., 1931, Phenomenal regression to the real object: British Journal of Psychology, v.21, p. 339-359.

U.S. Army, 1977, Shore Protection Manual, Coastal Engineering Research Center, 3 vols.

Walton, T. L., 1980, Computation of longshore energy flux using LEO current observations: U.S. Army Coastal Engineering Research Center, CETA No. 80-3.

Weggel, J. R., 1971, Statistical analysis of LEO breaker height observations: U.S. Army, Coastal Engineering Research Center, CEREN Memorandum for the Record, 30 Dec., 1971.